

Group-Sparse Smoothing for Longitudinal Models with Time-Varying Coefficients

Yu Lu¹, Tianni Zhang¹, Yuyao Wang¹, Mengfei Ran^{*1}

¹Wisdom Lake Academy of Pharmacy, Xi'an Jiaotong-Liverpool University

Abstract

Longitudinal data analysis is fundamental for understanding dynamic processes in biomedical and social sciences. Although varying coefficient models (VCMs) provide a flexible framework by allowing covariate effects to evolve over time, fitting all effects as time-varying may lead to overfitting, efficiency loss, and reduced interpretability when some effects are actually constant. In contrast, standard linear mixed models (LMMs) may suffer substantial bias when temporal heterogeneity is ignored. To address this issue, we propose time-varying effect selection, **TV-Select**, a unified framework for structural identification that simultaneously selects relevant variables and determines whether their effects are constant or time-varying. The proposed method decomposes each coefficient function into a time-invariant mean component and a centered time-varying deviation, where the latter is approximated by B-splines. We then construct a doubly penalized objective function that combines a group Lasso penalty for structural sparsity with a roughness penalty for smoothness control. An efficient block coordinate descent algorithm is developed for computation. Under regular semiparametric conditions, we establish selection consistency and oracle-type asymptotic properties, including asymptotic normality for the constant-effect component after correct structure recovery. Simulation studies and a real-data application show that TV-Select achieves more accurate structural recovery, smoother functional estimation, and better predictive performance than competing methods.

Keywords: Longitudinal data; Group Lasso; Varying coefficient models; Oracle property.

1 Introduction

Longitudinal studies collect repeated measurements on the same subjects and are central to modern biomedical, public-health, and social-science research. [Diggle et al. \(2002\)](#) gave a comprehensive account of modeling principles for longitudinal outcomes, while [Laird and Ware \(1982\)](#) established the random-effects framework that underlies linear mixed models for subject-specific heterogeneity. From a marginal perspective, [Liang and Zeger \(1986\)](#) introduced generalized estimating equations (GEE), which remain a cornerstone for population-level inference under working correlation structures.

A key limitation of constant-effect regression is that many covariate effects may evolve over time. To capture such dynamic associations, [Hastie and Tibshirani \(1993\)](#) introduced varying-coefficient models (VCMs), in which regression effects are allowed to change smoothly with time. Subsequent work developed both the statistical foundation and practical estimation tools for this class of models. For example, [Fan and Zhang \(1999\)](#) established statistical estimation theory for VCMs, [Hoover et al. \(1998\)](#) studied nonparametric smoothing estimators for longitudinal data, and [Wu and Zhang \(2006\)](#) provided a systematic treatment of nonparametric longitudinal

*Corresponding author. mengfei.ran@xjtlu.edu.cn

regression. Taken together, these developments strongly support flexible modeling of temporal heterogeneity, but they also highlight an important practical issue: in many applications, only a subset of predictors should genuinely vary with time, whereas others are constant or inactive.

This motivates structural identification in longitudinal VCMs, namely, determining whether each covariate is (i) irrelevant, (ii) constant, or (iii) time-varying. Penalization has become a major tool for this type of structure learning. The Lasso (Tibshirani, 1996) established a basic framework for sparse estimation, and the nonconcave penalization approach of Fan and Li (2001) provided oracle-type insights. For grouped structures, Yuan and Lin (2006) introduced the group Lasso, while Meier et al. (2008) extended blockwise penalties to generalized models, making exact group sparsity feasible. In the varying-coefficient setting, Wang et al. (2008) developed spline-based variable selection methods for nonparametric VCMs, and Wei et al. (2011) studied estimation and selection in high-dimensional VCMs with theoretical guarantees. Related work on additive models by Huang et al. (2010) complements this literature by emphasizing componentwise sparsity under basis expansions.

Smoothness control is equally important for interpretability. Classical spline approximation theory is well summarized by Schumaker (1981). For practical smoothing, Eilers and Marx (1996) developed P-splines by combining B-splines with roughness penalties, and Antoniadis et al. (2012) adapted this idea to variable selection in varying-coefficient models. More broadly, Stone (1985) studied additive regression and related structured nonparametric models, whereas Lin and Zhang (2006) emphasized that component selection and smoothing should be handled jointly rather than separately. These contributions suggest that a useful longitudinal VCM procedure should control both structural sparsity and functional regularity.

Several additional developments reinforce this perspective. Kai et al. (2011) studied efficient estimation and variable selection in semiparametric varying-coefficient partially linear models, and Xue et al. (2010) established consistent model selection for marginal generalized additive models. Beyond mean regression, Tang et al. (2013) considered variable selection in quantile varying-coefficient models, providing a complementary view of dynamic effects. Robustness is also important in practice: Zhao and Xue (2011) examined selection under measurement error, and Hu et al. (2021) investigated robust inference for varying-coefficient additive models. On the theoretical side, Lounici et al. (2011) derived oracle inequalities under group sparsity, offering a useful set of tools for analyzing block-penalized estimators.

High-dimensional longitudinal modeling has likewise developed rapidly. Wang et al. (2012) connected marginal modeling and sparsity through penalized GEE for high-dimensional longitudinal data. Inference for time-varying effects has also received growing attention: Chen and He (2018) studied inference in high-dimensional models with time-varying coefficients, and Dai and Kolar (2021) extended this line to high-dimensional varying-coefficient quantile regression. In related structured settings, Ke et al. (2016) investigated structure identification in panel data, while Li et al. (2015) considered model selection and structure specification in ultra-high dimensional generalized semi-varying coefficient models. At the same time, newer directions such as factor modeling (Bai and Ng, 2002), scalable Bayesian varying-coefficient models with unknown within-subject covariance (Bai et al., 2023), and deep-learning-based latent dynamic modeling (Köber et al., 2023) all point to the growing importance of interpretable structure-aware methodology. Related ideas also appear outside the longitudinal mean-regression setting; for instance, Hui et al. (2024) studied homogeneity pursuit and variable selection in multivariate abundance regression.

Against this background, we develop TV-Select, a unified framework for structural identification in longitudinal VCMs. The method is closely related to structure-learning ideas in panel and semi-varying coefficient models (Ke et al., 2016; Li et al., 2015), complements penalized marginal approaches for longitudinal data (Wang et al., 2012), and can be extended to adaptive weighting schemes (Zou, 2006; Wang and Leng, 2008) as well as robust inference settings (Hu et al., 2021). Its key device is to decompose each coefficient function into a time-invariant mean

component and a centered time-varying deviation, so that identifying time variation becomes equivalent to selecting nonzero deviation blocks. This formulation naturally connects spline approximation arguments (Schumaker, 1981) with group-sparsity theory (Lounici et al., 2011), and it is particularly well suited to applications where interpretability requires a clear distinction between constant and time-varying effects. Our empirical study is also designed to reflect standard benchmarks in the varying-coefficient literature (Wang et al., 2008; Wei et al., 2011), while remaining relevant to modern high-dimensional longitudinal modeling settings.

The rest of the paper is organized as follows. Section 2 introduces the model, the decomposition, and the doubly penalized estimator. Section 3 presents an efficient optimization algorithm based on block updates. Section 4 establishes estimation error bounds and structural recovery guarantees. Section 5 reports simulation studies across multiple scenarios and sample sizes. Section 6 illustrates the method on a real dataset with clearly documented provenance. Section 7 concludes with discussion and possible extensions.

2 Methodology

2.1 Longitudinal Model

Consider a longitudinal study with N subjects, for subject i ($i = 1, \dots, N$), we observe a response y_{ij} and a p -dimensional covariate vector $\mathbf{x}_{ij} = (x_{ij1}, \dots, x_{ijp})^\top$ at time t_{ij} , for $j = 1, \dots, n_i$. Let $\mathcal{T}_i = \{t_{i1}, \dots, t_{in_i}\}$ denote the observation times for subject i and $n = \sum_{i=1}^N n_i$ be the total number of observations. Without loss of generality, we assume that the observation times have been rescaled to $t_{ij} \in [0, 1]$ by a linear transformation.

From a modeling perspective it is natural, especially in longitudinal applications, to allow for subject-specific heterogeneity through a random intercept b_i . A convenient working model is

$$y_{ij} = \beta_0 + \sum_{k=1}^p \{\beta_k + f_k(t_{ij})\} x_{ijk} + b_i + \varepsilon_{ij},$$

where β_0 is a global intercept, β_k is the time-invariant main effect of the k -th covariate, $f_k(t)$ is a smooth time-varying deviation, b_i is a subject-specific random intercept with $\mathbb{E}(b_i) = 0$, and ε_{ij} are idiosyncratic errors with mean zero.

In practice, the random intercept b_i can be absorbed by a simple de-meaning step: for each subject i we subtract the subject-specific mean from both the response and the covariates,

$$\tilde{y}_{ij} = y_{ij} - \bar{y}_i, \quad \tilde{x}_{ijk} = x_{ijk} - \bar{x}_{ik},$$

where $\bar{y}_i = n_i^{-1} \sum_{j=1}^{n_i} y_{ij}$ and $\bar{x}_{ik} = n_i^{-1} \sum_{j=1}^{n_i} x_{ijk}$. The resulting model for $(\tilde{y}_{ij}, \tilde{\mathbf{x}}_{ij})$ has the same functional form as above with b_i removed. To simplify notation, in the remainder of the paper we continue to write $(y_{ij}, \mathbf{x}_{ij})$ for the de-measured quantities whenever the within-subject de-meaning step is applied; in that case the global intercept is redundant and can be set to $\beta_0 = 0$ (or estimated and will be close to zero). Alternatively, one may keep the original data without de-meaning, fit the working-independence model below, and account for within-subject correlation at the inference stage via cluster-robust (sandwich) standard errors. For theoretical development, we focus on the working-independence formulation

$$y_{ij} = \beta_0 + \sum_{k=1}^p x_{ijk} \beta_k(t_{ij}) + \varepsilon_{ij}, \tag{1}$$

where the time-varying coefficient functions $\beta_k(\cdot)$ are unknown smooth functions and ε_{ij} are independent errors with $\mathbb{E}(\varepsilon_{ij}) = 0$ and $\text{Var}(\varepsilon_{ij}) = \sigma^2$.

A key feature of TV-Select is that it does not assume a priori whether $\beta_k(t)$ is constant or

time-varying. Instead, we use a decomposition that separates a time-invariant mean effect from a centered time-varying deviation. For each $k = 1, \dots, p$, we write

$$\beta_k(t) = \mu_k + g_k(t), \quad \text{subject to } \int_0^1 g_k(t) dt = 0. \quad (2)$$

Here, μ_k denotes the time-invariant average effect of the k th covariate and $g_k(t)$ captures its time-varying deviation around this average. The centering constraint in (2) guarantees that the decomposition is unique and that μ_k has the natural interpretation of an average regression effect.

This decomposition induces a structural partition of the covariates into three disjoint sets:

$$\mathcal{S}_{\text{zero}} = \{k : \mu_k = 0, g_k(t) \equiv 0\}, \quad \mathcal{S}_{\text{const}} = \{k : \mu_k \neq 0, g_k(t) \equiv 0\}, \quad \mathcal{S}_{\text{vary}} = \{k : g_k(t) \not\equiv 0\}.$$

Variables in $\mathcal{S}_{\text{zero}}$ have no effect on the outcome, those in $\mathcal{S}_{\text{const}}$ contribute a constant (time-invariant) shift, and those in $\mathcal{S}_{\text{vary}}$ exhibit genuinely time-varying effects. The goal of TV-Select is to identify these sets and to estimate the corresponding functions $\beta_k(t)$ in a unified framework.

The representation in (1)–(2) naturally accommodates common longitudinal design features. Subject-specific baseline differences are captured by b_i and removed by de-meaning, while μ_k summarizes the overall effect of the k th covariate and $g_k(t)$ describes how this effect changes over time. Thus TV-Select simultaneously addresses variable selection and structural identification (constant vs. time-varying), which is crucial for interpretable longitudinal analysis.

2.2 Spline Approximation

To make the model in (1)–(2) estimable, we approximate the time-varying deviations $g_k(t)$ using B-spline basis functions. Let $\mathbb{S}_{q,d}$ be the space of B-spline functions of degree d with K internal knots $0 < \tau_1 < \dots < \tau_K < 1$. Let

$$\mathbf{B}(t) = (B_1(t), \dots, B_q(t))^\top, \quad q = K + d + 1,$$

denote the corresponding B-spline basis (Schumaker, 1981). Define the (unscaled) mean of each basis function by $\bar{B}_\ell = \int_0^1 B_\ell(u) du$ for $\ell = 1, \dots, q$. To enforce the zero-mean constraint in (2) and avoid collinearity between μ_k and $g_k(\cdot)$, we work with a centered basis

$$\tilde{B}_\ell(t) = B_\ell(t) - \bar{B}_\ell, \quad \ell = 1, \dots, q,$$

and write $\tilde{\mathbf{B}}(t) = (\tilde{B}_1(t), \dots, \tilde{B}_q(t))^\top$. We then approximate

$$g_k(t) \approx \tilde{\mathbf{B}}(t)^\top \boldsymbol{\theta}_k,$$

where $\boldsymbol{\theta}_k \in \mathbb{R}^q$ is the coefficient vector for the k th covariate.

Substituting $\beta_k(t) = \mu_k + g_k(t)$ and the spline approximation into (1) gives the approximating linear model

$$y_{ij} \approx \beta_0 + \sum_{k=1}^p x_{ijk} \mu_k + \sum_{k=1}^p x_{ijk} \tilde{\mathbf{B}}(t_{ij})^\top \boldsymbol{\theta}_k + \varepsilon_{ij}.$$

Let $\boldsymbol{\theta} = (\boldsymbol{\theta}_1^\top, \dots, \boldsymbol{\theta}_p^\top)^\top$ and define the group norm

$$\|\boldsymbol{\theta}\|_{2,1} = \sum_{k=1}^p \|\boldsymbol{\theta}_k\|_2,$$

as in grouped-variable selection (Yuan and Lin, 2006; Meier et al., 2008), so that

$$\Theta = (\beta_0, \mu_1, \dots, \mu_p, \boldsymbol{\theta}_1^\top, \dots, \boldsymbol{\theta}_p^\top)^\top$$

collect all parameters. For each k , define the $n \times q$ design matrix \mathbf{Z}_k whose (i, j) -th row is $\mathbf{z}_{ij,k}^\top = x_{ijk} \tilde{\mathbf{B}}(t_{ij})^\top$. Similarly, let \mathbf{X} be the $n \times p$ matrix stacking the covariate vectors \mathbf{x}_{ij} . Stacking all observations, the approximating model can be written compactly as

$$\mathbf{y} \approx \beta_0 \mathbf{1}_n + \mathbf{X}\boldsymbol{\mu} + \sum_{k=1}^p \mathbf{Z}_k \boldsymbol{\theta}_k + \boldsymbol{\varepsilon},$$

where \mathbf{y} and $\boldsymbol{\varepsilon}$ are the n -dimensional vectors of responses and errors, $\mathbf{1}$ is the n -dimensional vector of ones, and $\boldsymbol{\mu} = (\mu_1, \dots, \mu_p)^\top$.

2.3 Objective Function

We estimate $\Theta = (\beta_0, \mu_1, \dots, \mu_p, \boldsymbol{\theta}_1^\top, \dots, \boldsymbol{\theta}_p^\top)^\top$ by minimizing a doubly penalized least squares criterion. The empirical loss function is

$$L_N(\Theta) = \frac{1}{2} \sum_{i=1}^N \sum_{j=1}^{n_i} \left\{ y_{ij} - \beta_0 - \sum_{k=1}^p x_{ijk} (\mu_k + \tilde{\mathbf{B}}(t_{ij})^\top \boldsymbol{\theta}_k) \right\}^2.$$

The TV-Select estimator is defined as

$$\hat{\Theta} = \underset{\Theta}{\operatorname{argmin}} \left\{ L_N(\Theta) + \sum_{k=1}^p P_k(\boldsymbol{\theta}_k) \right\}, \quad (3)$$

where $P_k(\boldsymbol{\theta}_k)$ is a penalty applied to the spline coefficients of the k th covariate. We adopt the following doubly penalized structure:

$$P_k(\boldsymbol{\theta}_k) = \lambda_1 \|\boldsymbol{\theta}_k\|_2 + \lambda_2 \boldsymbol{\theta}_k^\top \boldsymbol{\Omega} \boldsymbol{\theta}_k, \quad (4)$$

with nonnegative tuning parameters λ_1 and λ_2 (possibly depending on N) and a positive semidefinite roughness matrix $\boldsymbol{\Omega}$.

The first component in (4), $\lambda_1 \|\boldsymbol{\theta}_k\|_2$, is a Group Lasso penalty, performs structural identification by shrinking entire deviation blocks to zero (Yuan and Lin, 2006). It treats $\boldsymbol{\theta}_k$ as a single group and shrinks the entire vector towards zero. For sufficiently large λ_1 , the solution satisfies $\|\hat{\boldsymbol{\theta}}_k\|_2 = 0$, implying $\hat{g}_k(t) \equiv 0$ and hence $\hat{\beta}_k(t) \equiv \hat{\mu}_k$ is time-invariant. The second component in (4), $\lambda_2 \boldsymbol{\theta}_k^\top \boldsymbol{\Omega} \boldsymbol{\theta}_k$, is a roughness penalty that enforces smoothness on the estimated time-varying component. In B-spline theory, a standard choice is

$$\boldsymbol{\Omega} = \int_0^1 \frac{d^2 \tilde{\mathbf{B}}(t)}{dt^2} \left\{ \frac{d^2 \tilde{\mathbf{B}}(t)}{dt^2} \right\}^\top dt,$$

which approximates the integrated squared second derivative of $g_k(t)$. The quadratic form $\boldsymbol{\theta}_k^\top \boldsymbol{\Omega} \boldsymbol{\theta}_k$ therefore penalizes excessive curvature in the estimated function.

The decomposition $\beta_k(t) = \mu_k + g_k(t)$ together with the doubly penalized criterion (3)–(4) is designed to recover the structural partition $(\mathcal{S}_{\text{zero}}, \mathcal{S}_{\text{const}}, \mathcal{S}_{\text{vary}})$. Time-varying predictors are identified by block selection on the deviation coefficients:

$$\hat{\mathcal{S}}_{\text{vary}} = \left\{ k : \|\hat{\boldsymbol{\theta}}_k\|_2 > 0 \right\}.$$

For any $k \notin \widehat{\mathcal{S}}_{\text{vary}}$, the estimated deviation satisfies $\hat{g}_k(t) \equiv 0$, hence $\hat{\beta}_k(t) \equiv \hat{\mu}_k$ is time-invariant. Because μ_k is not directly penalized in (3), exact zeros of $\hat{\mu}_k$ should not be expected in finite samples. We therefore distinguish constant effects from null effects among the non-time-varying predictors by thresholding $\hat{\mu}_k$. Specifically, for a threshold τ_N on the order of $\sqrt{\log(p)/n}$ (see Corollary 1),

$$\widehat{\mathcal{S}}_{\text{const}} = \left\{ k \notin \widehat{\mathcal{S}}_{\text{vary}} : |\hat{\mu}_k| > \tau_N \right\}, \quad \widehat{\mathcal{S}}_{\text{zero}} = \left\{ k \notin \widehat{\mathcal{S}}_{\text{vary}} : |\hat{\mu}_k| \leq \tau_N \right\}.$$

This yields a unified classification rule: detect time variation via $\|\hat{\boldsymbol{\theta}}_k\|_2 > 0$, and within the remaining predictors, separate constant versus null effects using $|\hat{\mu}_k|$ relative to τ_N .

Finally, the roughness penalty term $\lambda_2 \boldsymbol{\theta}_k^\top \boldsymbol{\Omega} \boldsymbol{\theta}_k$ ensures that whenever $k \in \widehat{\mathcal{S}}_{\text{vary}}$, the estimated deviation curve $\hat{g}_k(t) = \tilde{\mathbf{B}}(t)^\top \hat{\boldsymbol{\theta}}_k$ is smooth and interpretable, balancing parsimony (via group sparsity) and regularity (via smoothness) in structural identification for longitudinal data.

3 Algorithm

The objective function in (3) is convex but non-differentiable due to the group penalty $\lambda_1 \|\boldsymbol{\theta}_k\|_2$. We adopt a Block Coordinate Descent (BCD) strategy that alternates between (i) updating the constant effects $\{\mu_k\}$ (and the intercept if included) by least squares, and (ii) updating each time-varying block $\boldsymbol{\theta}_k$ via a two-step ‘‘smoothing + selection’’ update. This design mirrors the structural decomposition $\beta_k(t) = \mu_k + g_k(t)$: the first step targets μ_k and the second step decides whether $g_k(t)$ is identically zero.

Throughout, let $\mathbf{y} \in \mathbb{R}^n$ be the stacked response and $\mathbf{x}_k \in \mathbb{R}^n$ the stacked covariate column for predictor k . Denote $\tilde{\mathbf{B}}(t)$ be the centered spline basis and define the $n \times q$ block design matrix \mathbf{Z}_k whose rows are $\mathbf{z}_{ij,k}^\top = x_{ijk} \tilde{\mathbf{B}}(t_{ij})^\top$. We treat the intercept β_0 as optional: if within-subject de-meaning is applied, one may fix $\beta_0 = 0$.

3.1 Block updates

For intercept update. Given current $(\mu, \{\boldsymbol{\theta}_k\})$, the least-squares update is

$$\beta_0 \leftarrow \frac{1}{n} \mathbf{1}_n^\top \left(\mathbf{y} - \sum_{k=1}^p \mu_k \mathbf{x}_k - \sum_{k=1}^p \mathbf{Z}_k \boldsymbol{\theta}_k \right). \quad (5)$$

If an intercept is not used (e.g., after de-meaning), set $\beta_0 = 0$.

For constant effects update. Given the current $\{\mu_\ell\}_{\ell \neq k}$ and $\{\boldsymbol{\theta}_\ell\}_{\ell=1}^p$, define the partial residual

$$\mathbf{r}_\mu^{(k)} = \mathbf{y} - \beta_0 \mathbf{1}_n - \sum_{\ell \neq k} \mu_\ell \mathbf{x}_\ell - \sum_{\ell=1}^p \mathbf{Z}_\ell \boldsymbol{\theta}_\ell.$$

Then μ_k solves a one-dimensional least-squares problem and admits the closed-form update

$$\mu_k \leftarrow \frac{\mathbf{x}_k^\top \mathbf{r}_\mu^{(k)}}{\mathbf{x}_k^\top \mathbf{x}_k}. \quad (6)$$

Update of a for time-varying block update. Given current (β_0, μ) and $\{\boldsymbol{\theta}_\ell\}_{\ell \neq k}$, define

$$\mathbf{r}^{(k)} = \mathbf{y} - \beta_0 \mathbf{1}_n - \sum_{\ell=1}^p \mu_\ell \mathbf{x}_\ell - \sum_{\ell \neq k} \mathbf{Z}_\ell \boldsymbol{\theta}_\ell. \quad (7)$$

The k th block subproblem (with the same scaling as in (3)) is

$$\min_{\boldsymbol{\theta}_k \in \mathbb{R}^q} \frac{1}{2n} \|\mathbf{r}^{(k)} - \mathbf{Z}_k \boldsymbol{\theta}_k\|_2^2 + \lambda_2 \boldsymbol{\theta}_k^\top \boldsymbol{\Omega} \boldsymbol{\theta}_k + \lambda_1 \|\boldsymbol{\theta}_k\|_2. \quad (8)$$

Let

$$L_{\text{smooth}}(\boldsymbol{\theta}_k) = \frac{1}{2} \|\mathbf{r}^{(k)} - \mathbf{Z}_k \boldsymbol{\theta}_k\|_2^2 + \lambda_2 \boldsymbol{\theta}_k^\top \boldsymbol{\Omega} \boldsymbol{\theta}_k,$$

whose gradient is

$$\nabla L_{\text{smooth}}(\boldsymbol{\theta}_k) = -\mathbf{Z}_k^\top (\mathbf{r}^{(k)} - \mathbf{Z}_k \boldsymbol{\theta}_k) + 2\lambda_2 \boldsymbol{\Omega} \boldsymbol{\theta}_k. \quad (9)$$

A practical smoothing + selection update proceeds as follows.

(i) *Smoothing (ridge) step.* Compute the ridge-type estimate by minimizing the smooth part of (8):

$$\tilde{\boldsymbol{\theta}}_k = \arg \min_{\boldsymbol{\theta} \in \mathbb{R}^q} \left\{ \frac{1}{2n} \|\mathbf{r}^{(k)} - \mathbf{Z}_k \boldsymbol{\theta}\|_2^2 + \lambda_2 \boldsymbol{\theta}^\top \boldsymbol{\Omega} \boldsymbol{\theta} \right\} = \left(\frac{1}{n} \mathbf{Z}_k^\top \mathbf{Z}_k + 2\lambda_2 \boldsymbol{\Omega} \right)^{-1} \left(\frac{1}{n} \mathbf{Z}_k^\top \mathbf{r}^{(k)} \right). \quad (10)$$

The matrix $\frac{1}{n} \mathbf{Z}_k^\top \mathbf{Z}_k + 2\lambda_2 \boldsymbol{\Omega}$ does not depend on the residual and can be factorized once (e.g., Cholesky) for each k , which substantially reduces the per-iteration cost.

(ii) *Selection (group soft-thresholding) step.* Apply the proximal operator of the ℓ_2 -norm to induce block sparsity:

$$\boldsymbol{\theta}_k \leftarrow \mathcal{S}(\tilde{\boldsymbol{\theta}}_k, \lambda_1), \quad \mathcal{S}(\mathbf{v}, \lambda) = \left(1 - \frac{\lambda}{\|\mathbf{v}\|_2 + \varepsilon} \right)_+ \mathbf{v}, \quad (11)$$

where $\varepsilon > 0$ is a small constant for numerical stability and $(a)_+ = \max(a, 0)$. When $\|\tilde{\boldsymbol{\theta}}_k\|_2 \leq \lambda_1$, the update sets $\boldsymbol{\theta}_k = \mathbf{0}$, implying $\hat{g}_k(t) \equiv 0$ for predictor k . In implementations, one may optionally monitor the objective value and (if needed) damp the update to ensure monotone decrease.

3.2 Algorithm

Before running the iterations, we construct the centered spline basis $\tilde{\mathbf{B}}(\cdot)$ and the corresponding block design matrices $\{\mathbf{Z}_k\}_{k=1}^p$. In longitudinal applications, it is recommended to remove subject-specific baseline heterogeneity by within-subject de-meaning of the response and covariates, and to scale covariate columns if their magnitudes differ substantially. For computational efficiency, for each block k we precompute $\mathbf{G}_k = \mathbf{Z}_k^\top \mathbf{Z}_k / n$ and factorize $\mathbf{G}_k + 2\lambda_2 \boldsymbol{\Omega}$ once, so that the ridge step in (10) can be solved repeatedly via triangular solves.

Algorithm 1 Block Coordinate Descent with smoothing + selection updates

- 1: **Input:** Data $\{y_{ij}, \mathbf{x}_{ij}, t_{ij}\}$; centered basis $\tilde{\mathbf{B}}(\cdot)$; penalties λ_1, λ_2 ; tolerance ϵ ; maximum iterations T_{\max} .
 - 2: Construct \mathbf{y} , the covariate columns $\{\mathbf{x}_k\}_{k=1}^p$, and the design matrices $\{\mathbf{Z}_k\}_{k=1}^p$. For each k , compute $\mathbf{G}_k = \mathbf{Z}_k^\top \mathbf{Z}_k / n$ and factorize $\mathbf{G}_k + 2\lambda_2 \mathbf{\Omega}$.
 - 3: Initialize $\boldsymbol{\theta}_k^{(0)} = \mathbf{0}$ for all k and obtain $\mu^{(0)}$ by a constant-only least-squares fit. Initialize $\beta_0^{(0)}$ by (5) (or set $\beta_0^{(0)} = 0$ if no intercept). Compute the objective value $Q^{(0)}$.
 - 4: **for** $t = 0, 1, 2, \dots, T_{\max} - 1$ **do**
 - 5: Update $\beta_0^{(t+1)}$ by (5) (or keep $\beta_0^{(t+1)} = 0$ if no intercept).
 - 6: **for** $k = 1, \dots, p$ **do**
 - 7: Form $\mathbf{r}_\mu^{(k)} = \mathbf{y} - \beta_0^{(t+1)} \mathbf{1} - \sum_{\ell \neq k} \mu_\ell^{(t)} \mathbf{x}_\ell - \sum_{\ell=1}^p \mathbf{Z}_\ell \boldsymbol{\theta}_\ell^{(t)}$, then update $\mu_k^{(t+1)}$ by (6).
 - 8: **end for**
 - 9: **for** $k = 1, \dots, p$ **do**
 - 10: Form $\mathbf{r}^{(k)} = \mathbf{y} - \beta_0^{(t+1)} \mathbf{1} - \sum_{\ell=1}^p \mu_\ell^{(t+1)} \mathbf{x}_\ell - \sum_{\ell \neq k} \mathbf{Z}_\ell \boldsymbol{\theta}_\ell^{(t)}$.
 - 11: Solve the ridge smoothing step $\tilde{\boldsymbol{\theta}}_k$ by (10) using the factorization of $\mathbf{G}_k + 2\lambda_2 \mathbf{\Omega}$.
 - 12: Apply the group soft-thresholding step and set $\boldsymbol{\theta}_k^{(t+1)} \leftarrow \mathcal{S}(\tilde{\boldsymbol{\theta}}_k, \lambda_1)$ as in (11).
 - 13: **end for**
 - 14: Compute the new objective value $Q^{(t+1)}$.
 - 15: Stop if $|Q^{(t+1)} - Q^{(t)}| / (1 + Q^{(t)}) < \epsilon$.
 - 16: **end for**
 - 17: **Output:** $\{\hat{\mu}_k\}$ and $\{\hat{\boldsymbol{\theta}}_k\}$, and $\hat{\beta}_k(t) = \hat{\mu}_k + \tilde{\mathbf{B}}(t)^\top \hat{\boldsymbol{\theta}}_k$.
-

4 Asymptotic Properties

This section establishes estimation error bounds and structural identification guarantees for the doubly penalized estimator in (3)–(4). Recall the decomposition $\beta_k(t) = \mu_k + g_k(t)$ with $\int_0^1 g_k(t) dt = 0$ and the centered spline approximation $g_k(t) \approx \tilde{\mathbf{B}}(t)^\top \boldsymbol{\theta}_k$. Let $\mathcal{S}_{\text{vary}} = \{k : g_{0k}(\cdot) \not\equiv 0\}$, $\mathcal{S}_{\text{const}} = \{k : g_{0k}(\cdot) \equiv 0, \mu_{0k} \neq 0\}$, and $\mathcal{S}_{\text{zero}} = \{k : g_{0k}(\cdot) \equiv 0, \mu_{0k} = 0\}$, where μ_{0k} and $g_{0k}(\cdot)$ denote the true underlying effects. We focus on identification of $\mathcal{S}_{\text{vary}}$ through group sparsity of $\{\boldsymbol{\theta}_k\}$, and we treat identification of $\mathcal{S}_{\text{zero}}$ versus $\mathcal{S}_{\text{const}}$ via a simple thresholding step on $\hat{\mu}_k$ (see Corollary 1).

4.1 Assumptions

We assume the number of subjects $N \rightarrow \infty$. Let $n = \sum_{i=1}^N n_i$ and assume $\max_i n_i \leq \bar{n} < \infty$ for simplicity, so $n \asymp N$. All rates below can be rewritten in terms of n .

Assumption 1 (Design regularity and bounded moments). *The covariates satisfy $\mathbb{E}(x_{ijk}) = 0$ and are uniformly sub-Gaussian: there exists $K_x > 0$ such that $\sup_{i,j,k} \|x_{ijk}\|_{\psi_2} \leq K_x$. Moreover, the time points $t_{ij} \in [0, 1]$ are non-random or independent of ε_{ij} , and the centered spline basis $\tilde{\mathbf{B}}(t)$ is uniformly bounded in ℓ_∞ norm.*

Assumption 2 (Error distribution and working independence). *The errors ε_{ij} satisfy $\mathbb{E}(\varepsilon_{ij} \mid \{t_{i\ell}, \mathbf{x}_{i\ell}\}_{\ell=1}^{n_i}) = 0$ and are conditionally sub-Gaussian: $\sup_{i,j} \|\varepsilon_{ij}\|_{\psi_2} \leq K_\varepsilon$. For theoretical development we assume independence across (i, j) after de-meaning within subject (working independence); in longitudinal applications, inference may use cluster-robust standard errors.*

Assumption 3 (Smoothness and spline approximation). *For each $k \in \mathcal{S}_{\text{vary}}$, the true deviation function g_{0k} belongs to a Hölder class $\mathcal{H}_r([0, 1])$ with smoothness index $r > 2$. Let $q = q_N$ be the number of centered B-spline basis functions of degree $d \geq \lceil r \rceil - 1$. Then there exist spline coefficients $\boldsymbol{\theta}_{0k}^* \in \mathbb{R}^q$ such that $\sup_{t \in [0, 1]} |g_{0k}(t) - \tilde{\mathbf{B}}(t)^\top \boldsymbol{\theta}_{0k}^*| \leq Cq^{-r}$.*

Assumption 4 (Restricted eigenvalue / compatibility). Let $\mathbf{X} \in \mathbb{R}^{n \times p}$ be the design matrix for the constant effects and let $\mathbf{Z}_S \in \mathbb{R}^{n \times (s_v q)}$ be the concatenation of $\{\mathbf{Z}_k : k \in \mathcal{S}_{\text{vary}}\}$. There exists a constant $\kappa_0 > 0$ such that, with probability tending to one,

$$\frac{1}{n} \|\delta_0 \mathbf{1}_n + \mathbf{X}\delta_\mu + \mathbf{Z}_S \delta_\theta\|_2^2 \geq \kappa_0 (\delta_0^2 + \|\delta_\mu\|_2^2 + \|\delta_\theta\|_2^2)$$

for all $\delta_0 \in \mathbb{R}$, $\delta_\mu \in \mathbb{R}^p$, and $\delta_\theta \in \mathbb{R}^{s_v q}$.

Assumption 5 (Dimensionality and tuning). Let $s_v = |\mathcal{S}_{\text{vary}}|$ and assume $p + s_v q = o(n)$ and $\log p = o(n)$. Choose the group penalty level

$$\lambda_1 \asymp \sqrt{\frac{q \log p}{n}},$$

and take $\lambda_2 \geq 0$ either fixed or slowly varying with N such that $\|\boldsymbol{\Omega}\|_{\text{op}}$ is bounded and $\lambda_2 \|\boldsymbol{\Omega}\|_{\text{op}} = O(1)$.

Remark. Assumptions 1–2 provide concentration for empirical processes and justify the choice of λ_1 at the level $\sqrt{q \log(p)}/n$, which matches the typical size of $\max_k \|\mathbf{Z}_k^\top \boldsymbol{\varepsilon}\|_2/n$. Assumption 3 quantifies spline approximation error, enabling a bias–variance tradeoff via q . Assumption 4 ensures identifiability and controls ill-conditioning on the active subspace. Assumption 5 specifies the growth regime under which consistent estimation and selection are possible.

4.2 Results

Define $\boldsymbol{\theta}_{0k}^*$ as the spline approximation coefficients from Assumption 3 and let $\boldsymbol{\theta}_0^* = (\boldsymbol{\theta}_{01}^{*\top}, \dots, \boldsymbol{\theta}_{0p}^{*\top})^\top$ with $\boldsymbol{\theta}_{0k}^* = \mathbf{0}$ for $k \notin \mathcal{S}_{\text{vary}}$. Let $\boldsymbol{\mu}_0 = (\mu_{01}, \dots, \mu_{0p})^\top$ and denote the approximation error by

$$r_{ij} = \sum_{k \in \mathcal{S}_{\text{vary}}} x_{ijk} \left\{ g_{0k}(t_{ij}) - \tilde{\mathbf{B}}(t_{ij})^\top \boldsymbol{\theta}_{0k}^* \right\}.$$

Then the stacked model can be written as $\mathbf{y} = \beta_0 \mathbf{1}_n + \mathbf{X}\boldsymbol{\mu}_0 + \sum_{k=1}^p \mathbf{Z}_k \boldsymbol{\theta}_{0k}^* + \boldsymbol{\varepsilon} + \mathbf{r}$.

Theorem 1 (Estimation error and rate). Under Assumptions 1–5, with probability at least $1 - c_1 p^{-c_2}$, the estimator $(\hat{\beta}_0, \hat{\boldsymbol{\mu}}, \{\hat{\boldsymbol{\theta}}_k\})$ satisfies

$$\begin{aligned} \frac{1}{n} \left\| \mathbf{X}(\hat{\boldsymbol{\mu}} - \boldsymbol{\mu}_0) + \sum_{k=1}^p \mathbf{Z}_k (\hat{\boldsymbol{\theta}}_k - \boldsymbol{\theta}_{0k}^*) \right\|_2^2 &\leq C (s_v q \lambda_1^2 + s_v q^{-2r}), \\ \|\hat{\boldsymbol{\mu}} - \boldsymbol{\mu}_0\|_2^2 + \sum_{k \in \mathcal{S}_{\text{vary}}} \|\hat{\boldsymbol{\theta}}_k - \boldsymbol{\theta}_{0k}^*\|_2^2 &\leq C (s_v q \lambda_1^2 + s_v q^{-2r}), \end{aligned}$$

for constants $C, c_1, c_2 > 0$ independent of (N, p) . Consequently, for each $k \in \mathcal{S}_{\text{vary}}$, the estimated function $\hat{g}_k(t) = \tilde{\mathbf{B}}(t)^\top \hat{\boldsymbol{\theta}}_k$ obeys

$$\left(\int_0^1 \{\hat{g}_k(t) - g_{0k}(t)\}^2 dt \right)^{1/2} = O_p \left(q^{-r} + \sqrt{\frac{q \log p}{n}} \right).$$

In particular, choosing $q \asymp n^{1/(2r+1)}$ yields the near-optimal rate $O_p(n^{-r/(2r+1)} \sqrt{\log p})$.

The bound separates a spline approximation term q^{-r} (bias) from a high-dimensional estimation term $\sqrt{(q \log p)/n}$. The recommended $q \asymp n^{1/(2r+1)}$ balances these two terms and recovers the usual nonparametric rate up to the $\sqrt{\log p}$ factor induced by searching over p

groups. Moreover, λ_2 enters only through stability of the smooth component (via bounded operator norm assumptions) and does not change the leading-order rate as long as it is controlled as in Assumption 5.

Theorem 2 (Selection consistency for time-varying effects). *Assume Assumptions 1–5 and additionally the following two conditions:*

1. **Incoherence for inactive groups.** *There exists $\eta \in (0, 1)$ such that, with probability tending to one,*

$$\max_{k \notin \mathcal{S}_{\text{vary}}} \left\| \frac{1}{n} \mathbf{Z}_k^\top (\mathbf{I} - \mathbf{P}_{\mathbf{X}, \mathbf{Z}_S}) \mathbf{Z}_S (\mathbf{Z}_S^\top \mathbf{Z}_S)^{-1} \right\|_{\text{op}} \leq 1 - \eta,$$

where $\mathbf{P}_{\mathbf{X}, \mathbf{Z}_S}$ is the projection onto the column space of $[\mathbf{1}_n, \mathbf{X}, \mathbf{Z}_S]$.

2. **Beta-min (signal strength).** *There exists $c_0 > 0$ such that*

$$\min_{k \in \mathcal{S}_{\text{vary}}} \|\boldsymbol{\theta}_{0k}^*\|_2 \geq c_0 \lambda_1.$$

Then, letting $\widehat{\mathcal{S}}_{\text{vary}} = \{k : \|\widehat{\boldsymbol{\theta}}_k\|_2 > 0\}$, we have

$$\mathbb{P}(\widehat{\mathcal{S}}_{\text{vary}} = \mathcal{S}_{\text{vary}}) \rightarrow 1 \quad \text{as } N \rightarrow \infty.$$

Theorem 2 targets recovery of the time-varying set $\mathcal{S}_{\text{vary}}$ by exploiting group sparsity in the deviation blocks $\boldsymbol{\theta}_k$. The incoherence condition plays a role analogous to an irrepresentable-type requirement for group selection, ruling out excessive leakage of active deviation blocks into inactive ones after partialling out $[\mathbf{1}_n, \mathbf{X}, \mathbf{Z}_S]$. The beta-min condition ensures that true time variation is separated from noise at the scale λ_1 . Notably, this selection result is about whether $g_k(\cdot)$ is identically zero; it does not by itself separate $\mathcal{S}_{\text{const}}$ from $\mathcal{S}_{\text{zero}}$, which is handled by thresholding $\hat{\mu}_k$ in Corollary 1.

Corollary 1 (Consistent classification of $\mathcal{S}_{\text{zero}}$ vs $\mathcal{S}_{\text{const}}$). *Assume Theorem 2 holds so that $\widehat{\mathcal{S}}_{\text{vary}} = \mathcal{S}_{\text{vary}}$ with probability tending to one. Define a threshold τ_N with $\tau_N \asymp \sqrt{\log p/n}$ and classify*

$$\widehat{\mathcal{S}}_{\text{const}} = \left\{ k \notin \widehat{\mathcal{S}}_{\text{vary}} : |\hat{\mu}_k| > \tau_N \right\}, \quad \widehat{\mathcal{S}}_{\text{zero}} = \left\{ k \notin \widehat{\mathcal{S}}_{\text{vary}} : |\hat{\mu}_k| \leq \tau_N \right\}.$$

If additionally $\min_{k \in \mathcal{S}_{\text{const}}} |\mu_{0k}| \geq c_1 \tau_N$ for some $c_1 > 1$, then

$$\mathbb{P}(\widehat{\mathcal{S}}_{\text{const}} = \mathcal{S}_{\text{const}}, \widehat{\mathcal{S}}_{\text{zero}} = \mathcal{S}_{\text{zero}}) \rightarrow 1.$$

Because μ_k is not directly penalized in (3), we use a threshold τ_N to separate small estimation noise from genuinely nonzero constant effects. The scale $\tau_N \asymp \sqrt{\log(p)/n}$ matches the uniform (over p) stochastic fluctuation expected in high-dimensional settings. Practically, τ_N can be taken as a multiple of $\sqrt{\log(p)/n}$ or chosen by a stability/BIC-type rule; the corollary formalizes that a vanishing threshold (but not too fast) yields consistent classification provided constant signals exceed the threshold.

Theorem 3 (Oracle asymptotic normality for constant effects). *Assume Theorem 2 and suppose $|\mathcal{S}_{\text{const}}|$ is fixed. On the event $\widehat{\mathcal{S}}_{\text{vary}} = \mathcal{S}_{\text{vary}}$, consider the “oracle” estimator that solves (3) restricted to $\{\boldsymbol{\theta}_k = \mathbf{0} : k \notin \mathcal{S}_{\text{vary}}\}$. Then, for any fixed vector $\mathbf{a} \in \mathbb{R}^{|\mathcal{S}_{\text{const}}|}$,*

$$\sqrt{n} \mathbf{a}^\top (\hat{\mu}_{\mathcal{S}_{\text{const}}} - \mu_{0, \mathcal{S}_{\text{const}}}) \xrightarrow{d} \mathcal{N} \left(0, \sigma^2 \mathbf{a}^\top \left(\lim_{N \rightarrow \infty} \frac{1}{n} \mathbf{X}_{\mathcal{S}_{\text{const}}}^\top \mathbf{M} \mathbf{X}_{\mathcal{S}_{\text{const}}} \right)^{-1} \mathbf{a} \right),$$

where \mathbf{M} is the residual-maker that projects out $[\mathbf{1}_n, \mathbf{X}_{\mathcal{S}_{\text{vary}}}, \mathbf{Z}_{\mathcal{S}_{\text{vary}}}]$. Thus, $\hat{\mu}_{\mathcal{S}_{\text{const}}}$ is asymptotically as efficient as if the time-varying set were known in advance.

Theorem 3 is stated under the working-independence assumption used for estimation. In longitudinal applications with within-subject correlation, the same post-selection target can be paired with cluster-robust (sandwich) covariance estimation to obtain valid standard errors for the constant effects, while the selection step remains driven by detecting nonzero deviation blocks. The theorem formalizes the key message: once the time-varying set is correctly identified, estimation of constant effects proceeds as if the structural form were known a priori.

5 Numerical Study

We conduct extensive simulation studies to evaluate the proposed doubly penalized procedure in (i) estimation accuracy for both constant effects and time-varying deviations, (ii) structural identification of time-varying covariates, and (iii) prediction performance under a range of longitudinal data complexities. All simulations follow the model

$$y_{ij} = \beta_0 + \sum_{k=1}^p x_{ijk} \{\mu_{0k} + g_{0k}(t_{ij})\} + \varepsilon_{ij}, \quad \int_0^1 g_{0k}(t) dt = 0,$$

where $i = 1, \dots, N$ indexes subjects, $j = 1, \dots, n_i$ indexes repeated measurements, and $t_{ij} \in [0, 1]$. The centering constraint on g_{0k} ensures identifiability between μ_{0k} and $g_{0k}(\cdot)$ and matches our centered spline construction.

5.1 Data Generation

We consider both regular and irregular observation schedules. In the regular setting, each subject has $n_i \equiv n$ measurements at $t_{ij} = (j - 1)/(n - 1)$. In the irregular setting, $n_i \equiv n$ and t_{ij} are independently drawn from $\text{Unif}(0, 1)$ and then sorted within each subject.

Covariates are generated in two ways. In the baseline (time-invariant) design, each subject has $\mathbf{x}_i = (x_{i1}, \dots, x_{ip})^\top$ and we set $x_{ijk} = x_{ik}$ for all j . In the time-varying design, x_{ijk} changes over time according to $x_{ijk} = x_{ik} + \delta_{ijk}$ with $\delta_{ijk} \sim \mathcal{N}(0, \sigma_x^2)$ independently across (i, j, k) .

For the baseline component \mathbf{x}_i , we generate $\mathbf{x}_i \sim \mathcal{N}(\mathbf{0}, \boldsymbol{\Sigma})$ with $\Sigma_{k\ell} = \rho^{|k-\ell|}$ (AR(1)-type correlation), where $\rho \in \{0, 0.3, 0.6\}$ controls the predictor dependence. All covariates are standardized to have empirical mean zero and variance one before model fitting.

We partition predictors into three disjoint sets:

$$\begin{aligned} \mathcal{S}_{\text{vary}} &= \{k : g_{0k}(\cdot) \not\equiv 0\}, \\ \mathcal{S}_{\text{const}} &= \{k : g_{0k}(\cdot) \equiv 0, \mu_{0k} \neq 0\}, \\ \mathcal{S}_{\text{zero}} &= \{k : g_{0k}(\cdot) \equiv 0, \mu_{0k} = 0\}. \end{aligned}$$

Unless stated otherwise, we fix $s_v = |\mathcal{S}_{\text{vary}}| = 6$ and $s_c = |\mathcal{S}_{\text{const}}| = 6$. For constant effects, we set

$$\mu_{0k} = \begin{cases} 1.0, & k \in \mathcal{S}_{\text{const}}^{(1)}, \\ -1.0, & k \in \mathcal{S}_{\text{const}}^{(2)}, \\ 0, & k \in \mathcal{S}_{\text{vary}} \cup \mathcal{S}_{\text{zero}}, \end{cases}$$

where $\mathcal{S}_{\text{const}}^{(1)}$ and $\mathcal{S}_{\text{const}}^{(2)}$ split $\mathcal{S}_{\text{const}}$ evenly. The intercept is fixed at $\beta_0 = 0$.

For time-varying deviations, we specify $g_{0k}(t)$ for $k \in \mathcal{S}_{\text{vary}}$ using a mix of smooth patterns:

$$\begin{aligned}\tilde{g}_1(t) &= \sin(2\pi t), \\ \tilde{g}_2(t) &= \cos(2\pi t), \\ \tilde{g}_3(t) &= \sin(4\pi t), \\ \tilde{g}_4(t) &= \cos(4\pi t), \\ \tilde{g}_5(t) &= 16t^2(1-t)^2, \\ \tilde{g}_6(t) &= \sin(\pi t).\end{aligned}$$

and enforce the centering constraint by

$$g_{0k}(t) = a_k \left\{ \tilde{g}_k(t) - \int_0^1 \tilde{g}_k(u) du \right\}, \quad k \in \mathcal{S}_{\text{vary}}.$$

We set the amplitudes $a_k \in \{0.5, 1.0\}$ to control signal strength; the baseline setting uses $a_k = 1.0$. The inclusion of \tilde{g}_6 introduces a piecewise-constant deviation (mild non-smoothness) to test robustness to local irregularities.

Moreover, we consider the following error settings.

1. **Homoscedastic Gaussian:** $\varepsilon_{ij} \sim \mathcal{N}(0, \sigma^2)$ independently.
2. **Heavy-tailed:** $\varepsilon_{ij} \sim t_\nu$ scaled to have variance σ^2 with $\nu \in \{3, 5\}$.
3. **Heteroscedastic:** $\varepsilon_{ij} = \sigma(t_{ij}) \xi_{ij}$ where $\xi_{ij} \sim \mathcal{N}(0, 1)$ and $\sigma(t) = \sigma\{1 + 0.5 \sin(2\pi t)\}$.
4. **Within-subject correlation:** $\varepsilon_i = (\varepsilon_{i1}, \dots, \varepsilon_{in})^\top$ follows $\mathcal{N}(\mathbf{0}, \sigma^2 \mathbf{R})$ with $\mathbf{R}_{j\ell} = \alpha^{|j-\ell|}$ and $\alpha \in \{0.3, 0.6\}$.

Unless otherwise stated, we use $\sigma = 1$. When within-subject correlation is present, we still fit all methods under working independence (as in the paper) to assess robustness.

5.2 Simulation Scenarios

We evaluate six scenarios that progressively increase difficulty. Across scenarios, we vary (N, n, p) to reflect both moderate- and high-dimensional regimes. Unless stated otherwise, the spline basis uses cubic B-splines with q basis functions, where $q \in \{8, 10, 12\}$ increases slowly with sample size.

1. **Scenario A (baseline, independent, irregular time):** baseline covariates ($x_{ijk} = x_{ik}$), irregular t_{ij} , homoscedastic Gaussian errors, $\rho \in \{0, 0.3\}$. This scenario targets basic estimation and selection.
2. **Scenario B (correlated predictors):** same as Scenario A but with stronger predictor correlation $\rho = 0.6$. This scenario challenges identifiability and group selection under multicollinearity.
3. **Scenario C (within-subject correlation):** baseline covariates, regular time grid, AR(1) within-subject errors with $\alpha \in \{0.3, 0.6\}$. This scenario tests robustness to longitudinal dependence under working independence fitting.
4. **Scenario D (heavy-tailed and heteroscedastic errors):** baseline covariates, irregular time, errors follow either heavy-tailed t_ν (with $\nu = 3$) or heteroscedastic Gaussian. This scenario tests sensitivity to non-Gaussianity and non-constant variance.

5. **Scenario E (time-varying covariates):** time-varying covariates $x_{ijk} = x_{ik} + \delta_{ijk}$ with $\sigma_x^2 \in \{0.1, 0.5\}$, irregular time, Gaussian errors. This scenario checks stability when the covariates fluctuate over time.
6. **Scenario F (weaker time-varying signals and mild non-smoothness):** same as Scenario A but set $a_k = 0.5$ for all $k \in \mathcal{S}_{\text{vary}}$ and include \tilde{g}_6 . This scenario evaluates detection under low signal-to-noise and local non-smoothness.

We consider the following sample-size and dimensionality combinations:

$$(N, n_i, p) \in \{(100, 5, 100), (200, 5, 200), (200, 8, 200), (200, 8, 300)\}.$$

The total number of observations is $n = Nn_i$, each configuration is replicated $R = 200$ times. Reported results are averages over replications with Monte Carlo standard errors.

5.3 Competing Methods

We compare the proposed method (denoted **TV-Select**) against the following alternatives:

1. **Varying-coefficient without selection (VC-Ridge):** fit $\beta_k(t) = \mu_k + \tilde{\mathbf{B}}(t)^\top \boldsymbol{\theta}_k$ for all k with only the roughness penalty $\lambda_2 \sum_{k=1}^p \boldsymbol{\theta}_k^\top \boldsymbol{\Omega} \boldsymbol{\theta}_k$ (no group penalty). This method tests the benefit of structural selection.
2. **Group selection without roughness (Group-Lasso):** fit the same spline-augmented model but set $\lambda_2 = 0$ and penalize only $\sum_k \|\boldsymbol{\theta}_k\|_2$. This method isolates the role of the roughness penalty in stabilizing functional estimation.
3. **Two-stage screening and refit (Screen-Refit):** first fit Group-Lasso to select $\hat{\mathcal{S}}_{\text{vary}}$, then refit an unpenalized spline model on the selected blocks (with a mild ridge penalty for numerical stability). This method reflects a common pragmatic pipeline.

All methods use the same centered spline basis and the same q to ensure comparability.

5.4 Tuning Parameter

For the TV-Select, (λ_1, λ_2) are selected over a two-dimensional grid. We use an extended BIC-type criterion tailored to group sparsity:

$$\text{EBIC}(\lambda_1, \lambda_2) = \log \left(\frac{1}{n} \text{RSS} \right) + \frac{\log(n)}{n} \text{df} + \frac{2\gamma \log(p)}{n} |\hat{\mathcal{S}}_{\text{vary}}|,$$

where $\text{RSS} = \|\mathbf{y} - \hat{\beta}_0 \mathbf{1}_n - \mathbf{X} \hat{\boldsymbol{\mu}} - \sum_k \mathbf{Z}_k \hat{\boldsymbol{\theta}}_k\|_2^2$, df is an effective degrees-of-freedom proxy (taken as $p + q|\hat{\mathcal{S}}_{\text{vary}}|$), and $\gamma \in [0, 1]$ controls the strength of the extra dimensionality penalty; we use $\gamma = 0.5$ unless otherwise stated. For fairness, Group-Lasso and VC-Ridge use the same EBIC with their respective parameter grids. As a sensitivity check, we also experimented with K -fold cross-validation ($K = 5$), obtaining qualitatively similar conclusions.

The proposed algorithm is initialized at $\boldsymbol{\theta}_k = \mathbf{0}$ and $\boldsymbol{\mu}$ from the constant-only fit. We terminate iterations when the relative objective decrease falls below 10^{-6} or the iteration count exceeds 500.

5.5 Evaluation Metrics

For each replication, we compute metrics for function estimation, constant-effect estimation, structural identification, prediction performance, and the additional smoothness and stability properties that are central to the proposed doubly penalized procedure.

- **Estimation accuracy**

For each k , define

$$\hat{\beta}_k(t) = \hat{\mu}_k + \tilde{\mathbf{B}}(t)^\top \hat{\boldsymbol{\theta}}_k.$$

We measure functional estimation error on a dense grid $\{t_g\}_{g=1}^G$ with $G = 200$:

$$\text{ISE}_k = \frac{1}{G} \sum_{g=1}^G \{\hat{\beta}_k(t_g) - \beta_{0k}(t_g)\}^2, \quad \text{ISE} = \frac{1}{p} \sum_{k=1}^p \text{ISE}_k.$$

For constant effects, we report

$$\text{MSE}_\mu = \frac{\|\hat{\mu} - \mu_0\|_2^2}{p}, \quad \text{MSE}_{\mu, \text{act}} = \frac{\|\hat{\mu}_{\mathcal{S}_{\text{const}}} - \mu_{0, \mathcal{S}_{\text{const}}}\|_2^2}{s_c}.$$

To further assess the smoothness recovery of the estimated varying effects, we also compute the roughness error

$$\text{RE} = \frac{1}{|\mathcal{S}_{\text{vary}}|} \sum_{k \in \mathcal{S}_{\text{vary}}} \int_0^1 \{\hat{g}_k''(t) - g_{0k}''(t)\}^2 dt,$$

where $\hat{g}_k(t) = \tilde{\mathbf{B}}(t)^\top \hat{\boldsymbol{\theta}}_k$. This metric is particularly useful for highlighting the advantage of the roughness penalty in recovering smooth functional shapes.

- **Structural identification accuracy**

We evaluate selection of time-varying predictors via

$$\hat{\mathcal{S}}_{\text{vary}} = \{k : \|\hat{\boldsymbol{\theta}}_k\|_2 > 0\}.$$

We report

$$\text{TPR}_{\text{vary}} = \frac{|\hat{\mathcal{S}}_{\text{vary}} \cap \mathcal{S}_{\text{vary}}|}{|\mathcal{S}_{\text{vary}}|}, \quad \text{FPR}_{\text{vary}} = \frac{|\hat{\mathcal{S}}_{\text{vary}} \cap \mathcal{S}_{\text{vary}}^c|}{|\mathcal{S}_{\text{vary}}^c|}.$$

To further distinguish $\mathcal{S}_{\text{zero}}$ and $\mathcal{S}_{\text{const}}$, we apply the threshold rule $|\hat{\mu}_k| > \tau_N$ on $k \notin \hat{\mathcal{S}}_{\text{vary}}$ with $\tau_N = \sqrt{\log(p)/n}$, and compute the corresponding classification accuracy. Moreover, letting $\hat{c}_k \in \{\text{zero}, \text{const}, \text{vary}\}$ denote the estimated class of predictor k and $c_k \in \{\text{zero}, \text{const}, \text{vary}\}$ the true class, we report the overall three-way classification accuracy

$$\text{ClassAcc} = \frac{1}{p} \sum_{k=1}^p \mathbf{1}(\hat{c}_k = c_k),$$

which directly reflects the ability of the method to recover the full structural partition $(\mathcal{S}_{\text{zero}}, \mathcal{S}_{\text{const}}, \mathcal{S}_{\text{vary}})$.

Finally, to quantify the stability of time-varying set recovery across replications, we compute the average Jaccard index

$$\text{Stab} = \frac{2}{R(R-1)} \sum_{1 \leq r < s \leq R} \frac{|\hat{\mathcal{S}}_{\text{vary}}^{(r)} \cap \hat{\mathcal{S}}_{\text{vary}}^{(s)}|}{|\hat{\mathcal{S}}_{\text{vary}}^{(r)} \cup \hat{\mathcal{S}}_{\text{vary}}^{(s)}|}.$$

A larger value of Stab indicates that the selected time-varying set is more stable across repeated simulations.

- **Prediction performance**

We generate an independent test set with $N_{\text{test}} = 500$ subjects under the same DGP and compute the mean squared prediction error

$$\text{MSPE} = \frac{1}{n_{\text{test}}} \left\| \mathbf{y}_{\text{test}} - \hat{\beta}_0 \mathbf{1} - \mathbf{X}_{\text{test}} \hat{\mu} - \sum_{k=1}^p \mathbf{Z}_{k,\text{test}} \hat{\theta}_k \right\|_2^2.$$

5.6 Main Results

The simulation results in Table 1 show a clear and systematic advantage of the TV-Select across all scenarios and sample-size configurations. Overall, the proposed estimator delivers the most favorable balance among structural recovery, functional estimation, and prediction. In nearly all settings, it produces the smallest values of MSE_{μ} , $\text{MSE}_{\mu,\text{act}}$, MSPE, and RE, indicating that the doubly penalized formulation improves both estimation accuracy and smoothness recovery. This pattern is well aligned with the statistical design of the method: the group penalty controls unnecessary time variation by shrinking entire deviation blocks toward zero, while the roughness penalty regularizes the selected functional components and reduces variance inflation caused by flexible spline expansions.

The advantage in estimating constant effects is particularly stable across Scenarios A–F. The TV-Select consistently attains the smallest MSE_{μ} and $\text{MSE}_{\mu,\text{act}}$, which suggests that the decomposition $\beta_k(t) = \mu_k + g_k(t)$ is beneficial not only for structure identification but also for improving estimation of the time-invariant component itself. Statistically, this is because the proposed estimator borrows strength across the constant and varying parts while avoiding the unnecessary inflation of functional degrees of freedom. By contrast, VC-Ridge allows all predictors to vary over time and therefore tends to absorb part of the constant signal into noisy functional deviations, which increases estimation error. Group-Lasso improves structural sparsity but lacks an explicit smoothness constraint, so the estimated varying components remain unstable and can contaminate the estimation of μ_k . Screen+Refit is generally more competitive, but the two-stage nature of the procedure propagates screening error into the refitting step and loses the efficiency gain of solving the problem jointly.

Figure 1: ClassAcc across different configurations.

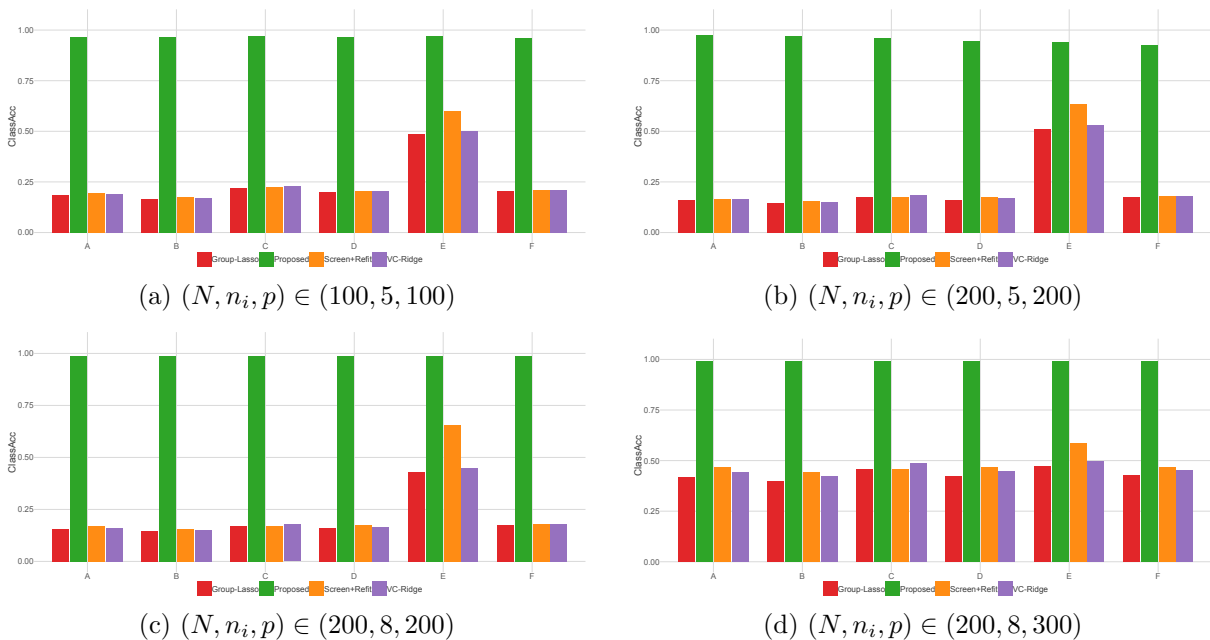


Table 1: Simulation results across scenarios and sample sizes.

Scenario	Method	$(N, n_i, p) \in (100, 5, 100)$					$(N, n_i, p) \in (200, 5, 200)$					$(N, n_i, p) \in (200, 8, 200)$					$(N, n_i, p) \in (200, 8, 300)$				
		MSE $_{\mu}$	MSE $_{\mu,act}$	MSPE	RE	MSE $_{\mu}$	MSE $_{\mu,act}$	MSPE	RE	MSE $_{\mu}$	MSE $_{\mu,act}$	MSPE	RE	MSE $_{\mu}$	MSE $_{\mu,act}$	MSPE	RE	MSE $_{\mu}$	MSE $_{\mu,act}$	MSPE	RE
A	TV-Select	0.0042	0.0688	2.3838	1.4233	0.0012	0.0397	1.8366	1.0402	0.0008	0.0250	1.7243	0.9513	0.0005	0.0252	1.5227	0.8082	0.0005	0.0252	1.5227	0.8082
	VC-Ridge	0.3603	0.3707	41.5937	447.5781	0.1812	0.1956	39.8947	243.9776	0.1158	0.1125	31.1826	300.6287	0.0096	0.0871	12.7004	235.7026	0.0096	0.0871	12.7004	235.7026
	Group-Lasso	0.3603	0.3707	41.5937	407.8863	0.1812	0.1956	39.8947	226.9203	0.1158	0.1125	31.1826	277.4924	0.0096	0.0871	12.7004	221.9360	0.0096	0.0871	12.7004	221.9360
	Screen+Refit	0.3358	0.3337	31.8061	27.2423	0.1615	0.1780	29.7953	13.5919	0.1011	0.0976	19.0935	9.4440	0.0077	0.0869	4.8147	11.7059	0.0077	0.0869	4.8147	11.7059
B	TV-Select	0.0076	0.1228	2.3498	1.5154	0.0013	0.0422	1.7300	1.2993	0.0010	0.0331	1.6745	1.2274	0.0008	0.0417	1.5524	1.1753	0.0008	0.0417	1.5524	1.1753
	VC-Ridge	0.4370	0.4626	30.8478	527.0499	0.2212	0.2142	29.7490	277.4416	0.1339	0.1293	22.5000	343.1390	0.0104	0.0741	11.5884	256.2138	0.0104	0.0741	11.5884	256.2138
	Group-Lasso	0.4370	0.4626	30.8478	475.1234	0.2212	0.2142	29.7490	257.4987	0.1339	0.1293	22.5000	314.1502	0.0104	0.0741	11.5884	240.2294	0.0104	0.0741	11.5884	240.2294
	Screen+Refit	0.4036	0.4389	22.3559	25.5322	0.1997	0.1991	21.7257	14.2350	0.1191	0.1164	13.3974	9.2241	0.0083	0.0710	4.2716	11.2593	0.0083	0.0710	4.2716	11.2593
C	TV-Select	0.0067	0.1086	2.2045	1.3919	0.0015	0.0507	1.7324	1.3594	0.0013	0.0441	1.6986	0.9134	0.0007	0.0348	1.6450	0.9774	0.0007	0.0348	1.6450	0.9774
	VC-Ridge	0.2877	0.2736	28.9443	9.5947	0.1533	0.1460	31.1039	5.3203	0.1137	0.1098	25.6883	14.0555	0.0085	0.0891	5.1977	4.4380	0.0085	0.0891	5.1977	4.4380
	Group-Lasso	0.2877	0.2736	28.9443	8.7432	0.1533	0.1460	31.1039	5.0928	0.1137	0.1098	25.6883	13.0826	0.0085	0.0891	5.1977	4.2375	0.0085	0.0891	5.1977	4.2375
	Screen+Refit	0.2782	0.2647	24.3092	1.5795	0.1481	0.1412	26.2204	1.4473	0.1097	0.1061	19.6903	1.0625	0.0085	0.0891	3.9292	1.2391	0.0085	0.0891	3.9292	1.2391
D	TV-Select	0.0046	0.0751	2.4041	1.4266	0.0010	0.0313	1.8340	1.0784	0.0009	0.0283	1.8247	0.9431	0.0004	0.0180	1.5475	0.8199	0.0004	0.0180	1.5475	0.8199
	VC-Ridge	0.3379	0.3673	45.6199	796.5322	0.1774	0.1742	38.9172	242.7978	0.1075	0.1080	29.5045	290.1352	0.0097	0.0892	12.5513	231.4365	0.0097	0.0892	12.5513	231.4365
	Group-Lasso	0.3379	0.3673	45.6199	716.8684	0.1774	0.1742	38.9172	226.5074	0.1075	0.1080	29.5045	268.0164	0.0097	0.0892	12.5513	218.2821	0.0097	0.0892	12.5513	218.2821
	Screen+Refit	0.3033	0.3123	28.9909	27.9820	0.1571	0.1566	29.1607	14.5313	0.0933	0.0925	17.7890	9.2850	0.0078	0.0874	4.8799	11.6325	0.0078	0.0874	4.8799	11.6325
E	TV-Select	0.0025	0.0406	2.4919	1.3431	0.0007	0.0235	1.8452	0.8720	0.0008	0.0253	1.8602	0.8143	0.0004	0.0182	1.5568	0.7014	0.0004	0.0182	1.5568	0.7014
	VC-Ridge	0.0186	0.0361	9.1849	283.0420	0.0082	0.0222	6.0601	91.3698	0.0077	0.0225	13.1551	309.4821	0.0064	0.0212	6.0830	78.5027	0.0064	0.0212	6.0830	78.5027
	Group-Lasso	0.0186	0.0361	9.1849	257.7132	0.0082	0.0222	6.0601	85.3775	0.0077	0.0225	13.1551	288.3140	0.0064	0.0212	6.0830	74.4106	0.0064	0.0212	6.0830	74.4106
	Screen+Refit	0.0106	0.0274	3.5493	23.0594	0.0046	0.0191	2.9831	14.9666	0.0026	0.0172	2.3330	9.3286	0.0036	0.0186	3.2312	14.4984	0.0036	0.0186	3.2312	14.4984
F	TV-Select	0.0041	0.0666	1.9752	1.4576	0.0011	0.0360	1.5985	1.1910	0.0010	0.0325	1.5641	1.0996	0.0003	0.0170	1.4009	0.9790	0.0003	0.0170	1.4009	0.9790
	VC-Ridge	0.2251	0.2318	30.0770	492.1595	0.1181	0.1244	28.4739	294.0993	0.0761	0.0804	23.6546	343.0244	0.0091	0.0890	12.1190	308.7988	0.0091	0.0890	12.1190	308.7988
	Group-Lasso	0.2251	0.2318	30.0770	453.0037	0.1181	0.1244	28.4739	274.0124	0.0761	0.0804	23.6546	322.5015	0.0091	0.0890	12.1190	294.1870	0.0091	0.0890	12.1190	294.1870
	Screen+Refit	0.2160	0.2311	21.3630	25.8805	0.1121	0.1174	21.6134	16.5631	0.0705	0.0752	13.9096	11.3109	0.0077	0.0873	4.8703	15.1795	0.0077	0.0873	4.8703	15.1795

Figure 2: TPR across different configurations.

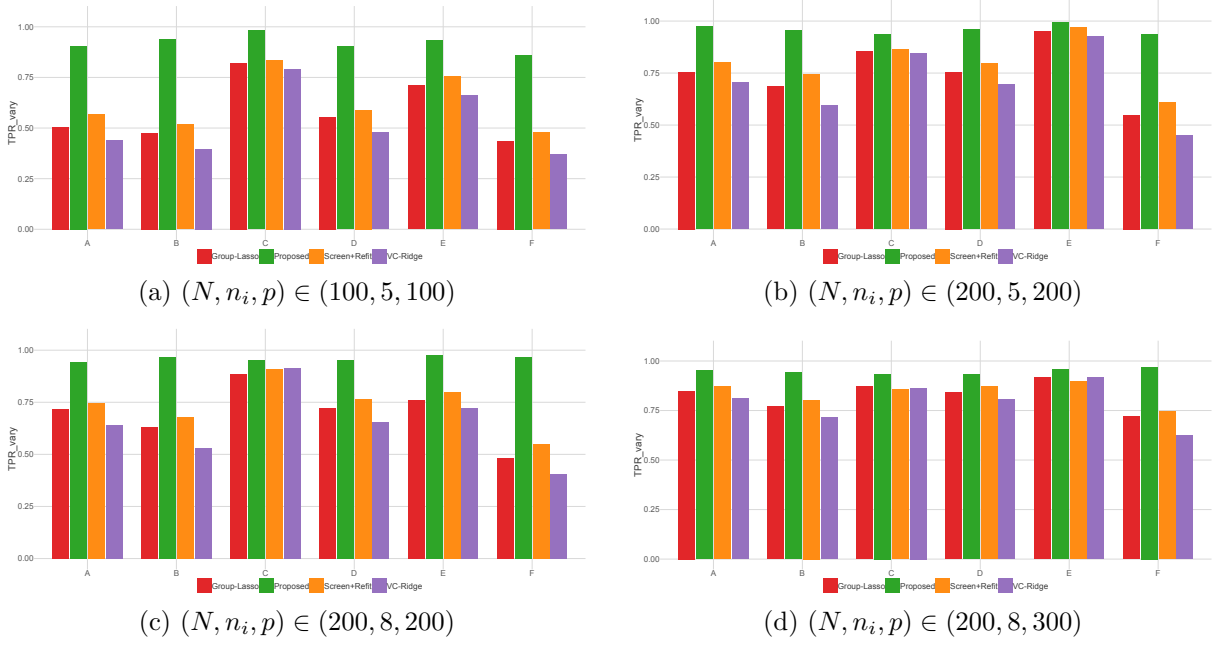


Figure 3: FPR across different configurations.

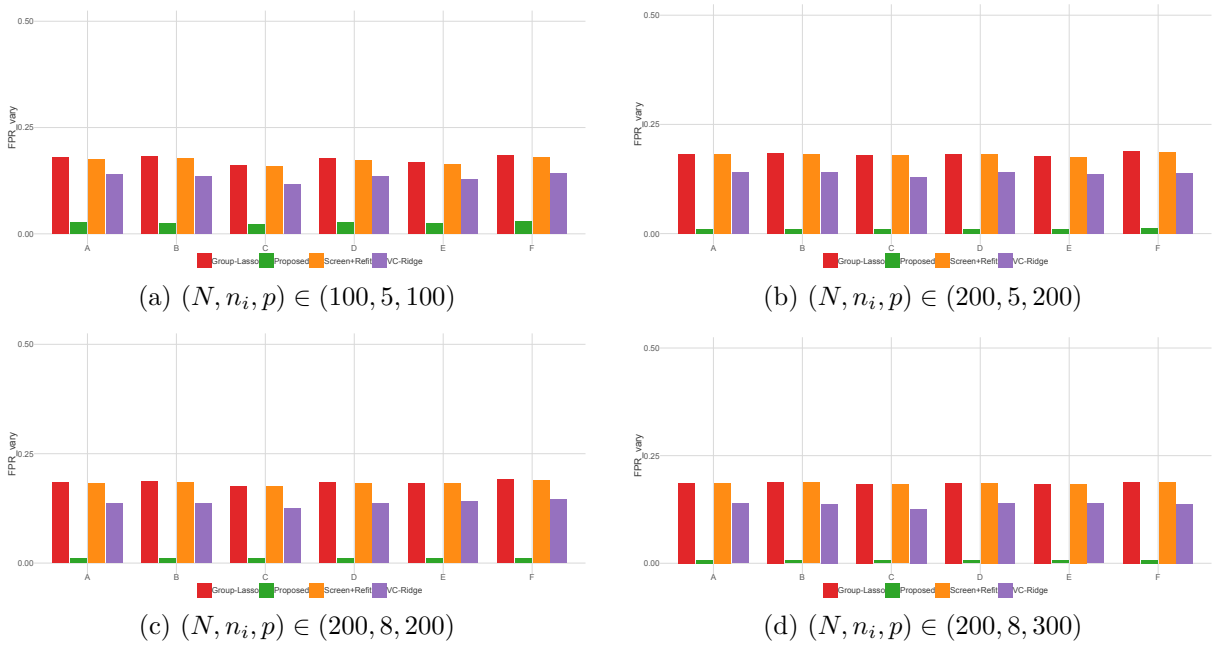


Figure 4: Stability across different configurations.

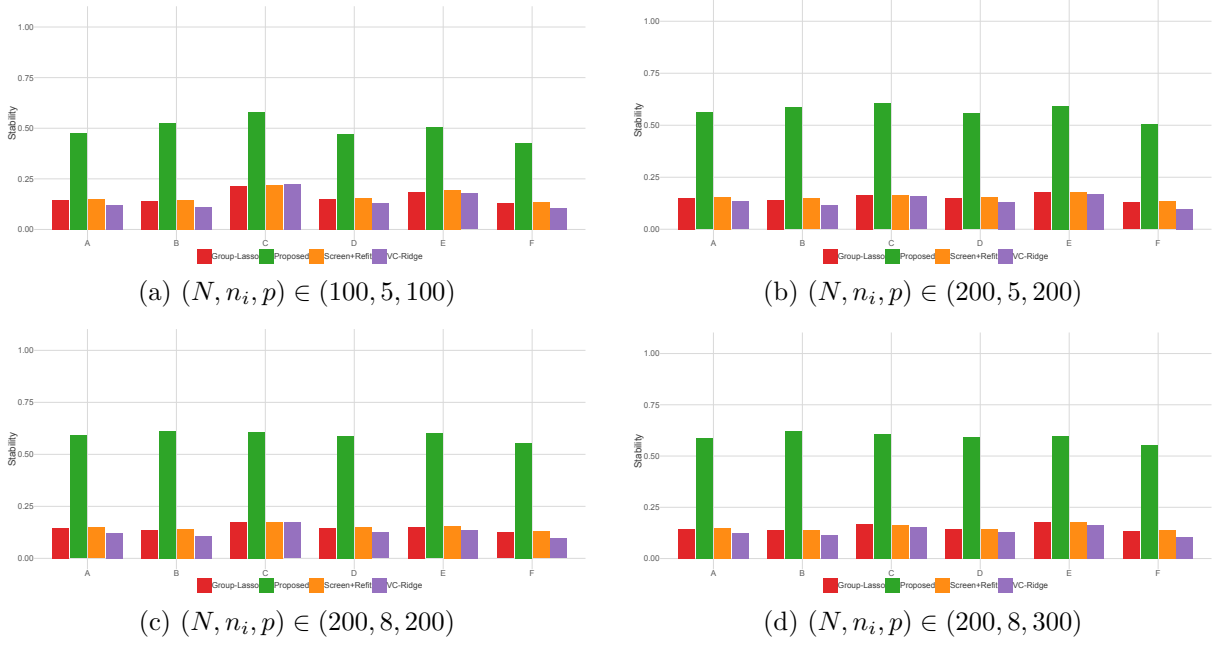
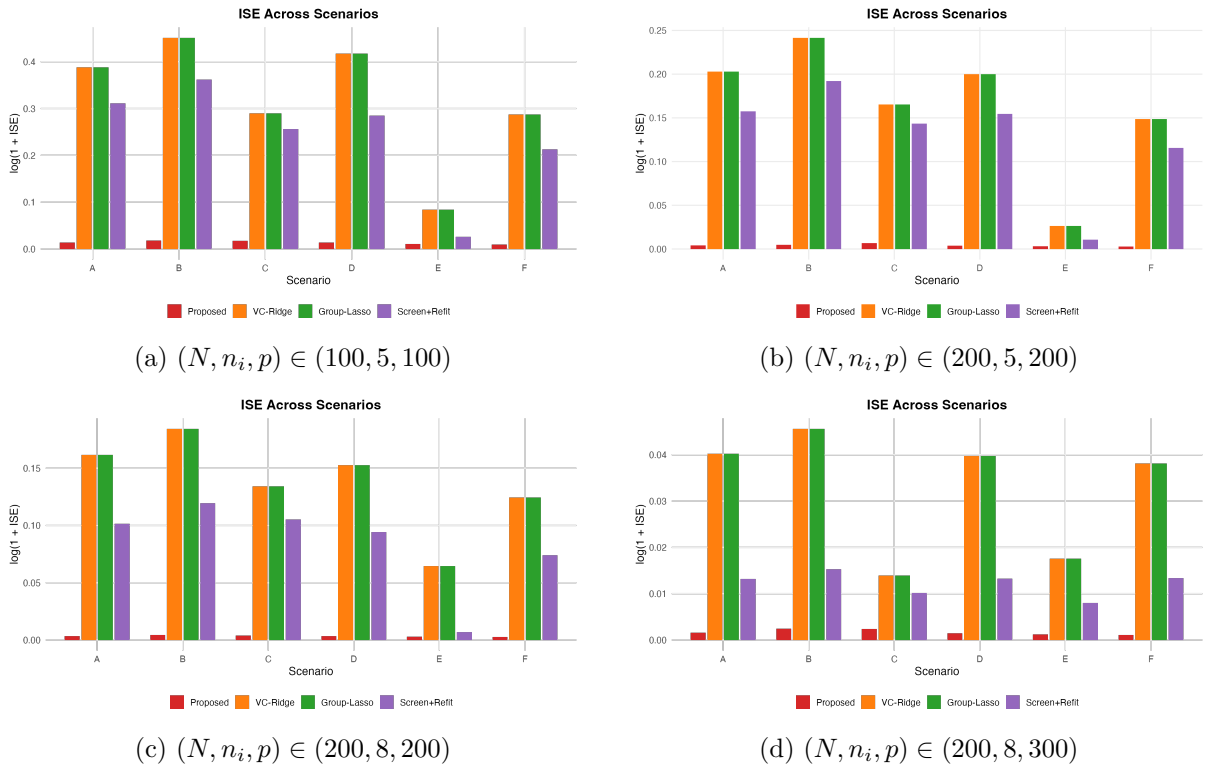


Figure 5: ISE across different configurations.



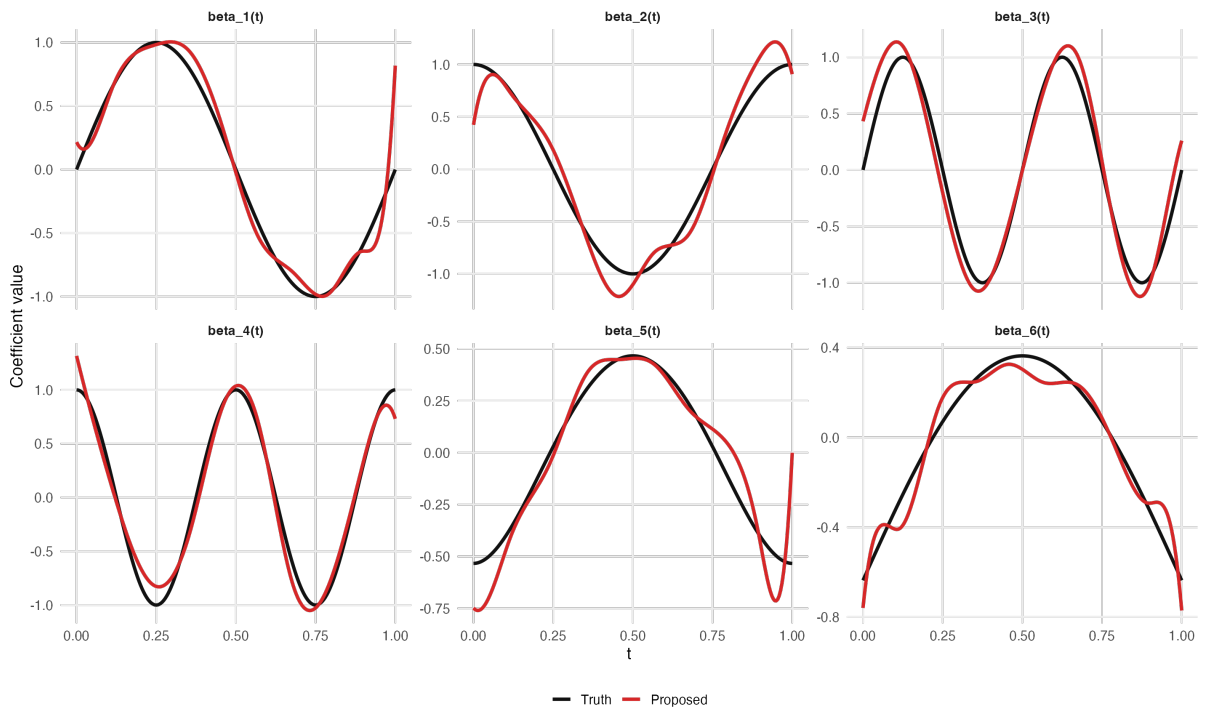


Figure 6: Estimated coefficient curves, configuration $(N, m, p) = (200, 8, 300)$ for Scenarios B.

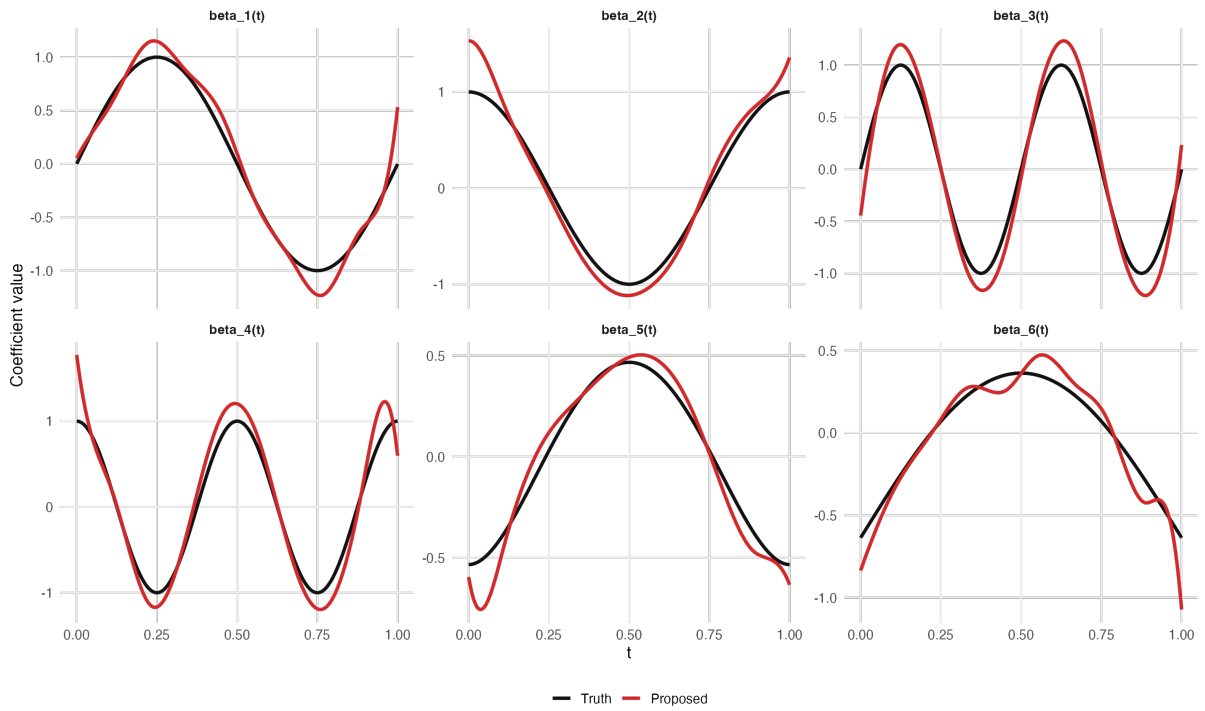


Figure 7: Estimated coefficient curves, configuration $(N, m, p) = (200, 8, 300)$ for Scenarios E.

A similar pattern appears in prediction. TV-Select uniformly yields the smallest or nearly smallest MSPE, and the gain becomes especially visible in the more challenging scenarios. This is again consistent with the underlying bias–variance tradeoff. Methods without selection, such as VC-Ridge, suffer from excessive variance because they estimate too many functional components. Methods without smoothness control, such as Group-Lasso, can fit irregular curves that track noise rather than the underlying signal, which also harms out-of-sample prediction. The proposed procedure reduces both sources of instability: sparsity limits overfitting at the model-selection level, and smoothness control stabilizes the nonzero curves at the estimation level.

The roughness results provide the clearest evidence for the role of the second penalty. Across all scenarios and all (N, m, p) combinations, TV-Select has dramatically smaller RE than the competing procedures. This confirms that the penalty $\lambda_2 \boldsymbol{\theta}_k^\top \boldsymbol{\Omega} \boldsymbol{\theta}_k$ is doing more than numerical smoothing: it effectively suppresses spurious oscillations generated by high-dimensional spline fitting, while preserving the dominant temporal structure of the true coefficient functions. In contrast, the very large roughness errors of VC-Ridge and Group-Lasso indicate that sparsity alone is insufficient for stable functional recovery. This is precisely the setting anticipated by the theory in Section 4, where the error bound contains both an approximation component and a stochastic component; the roughness penalty reduces the practical impact of the latter by regularizing the selected spline coefficients.

The structural recovery metrics show a consistency. TV-Select generally achieves the highest TPR_{vary} , while maintaining low false discovery and a large exact-recovery count. The additional measures ClassAcc and Stab further reinforce this conclusion. In nearly every setting, the proposed method has the best or nearly best three-way classification accuracy, showing that it can reliably distinguish zero, constant, and time-varying effects rather than merely separating varying from non-varying predictors. It also exhibits much larger stability across replications, which means that the selected time-varying set is far less sensitive to sampling fluctuation. This stability is not accidental: it is a direct consequence of combining block sparsity with smoothness regularization, which reduces the tendency of the procedure to switch variables in and out of the active varying set due to small local perturbations in the data.

The behavior across scenarios is also statistically meaningful. In the baseline settings, TV-Select already dominates the alternatives, showing that its benefit is not restricted to artificially difficult regimes. In Scenario C, where all methods perform better, the proposed estimator remains best or tied for best, indicating that the additional smoothness penalty does not sacrifice efficiency when the signal is relatively easy to recover. In the more demanding settings, such as those with stronger dependence, weaker signals, or more challenging covariate structures, the performance gap becomes more pronounced. This is exactly where the theoretical strengths of the proposed approach should matter most: stronger regularization is valuable when the estimation problem is less well-conditioned, and the simulation results confirm that this advantage carries over to finite samples.

The estimated coefficient curves provide a visual explanation for the numerical comparisons. Because of space limitations, Figures 6 and 7 display the six fitted coefficient curves only for the representative configuration $(N, m, p) = (200, 8, 300)$. Even under this moderately high-dimensional setting, the proposed curves track the true functional shapes closely across all scenarios. In the easier scenarios, the fitted curves are almost indistinguishable from the truth except for minor boundary deviations. In the more difficult scenarios, some discrepancy is unavoidable, but the TV-Select still captures the main peaks, troughs, and global trends without introducing unnecessary oscillation. This visual evidence is fully consistent with the much smaller roughness error and improved prediction accuracy reported in Table 1.

Taken together, the simulation study shows that the TV-Select achieves the most favorable compromise among structure identification, estimation accuracy, smoothness, prediction, and stability. These gains are not merely empirical: they reflect the statistical role of the two penal-

ties in controlling model complexity at two complementary levels—selection of which effects are allowed to vary, and regularization of how the selected effects are allowed to vary over time.

5.7 Summary

Overall, the numerical results demonstrate that TV-Select provides the most balanced performance across structural identification, functional estimation, smoothness recovery, and prediction. Compared with the competing procedures, it more accurately distinguishes zero, constant, and time-varying effects, yields substantially smoother coefficient estimates, and achieves consistently better predictive accuracy across a wide range of scenarios and sample-size settings. These findings confirm that the combination of group sparsity and roughness regularization is essential for stable and interpretable estimation in longitudinal varying-coefficient models.

6 Real Data Analysis

To assess the practical utility of the TV-Select, we analyzed the `sleep-cassette` subset from the publicly available Sleep-EDF Expanded database on PhysioNet¹ website. This dataset contains overnight polysomnography (PSG) recordings together with manually scored sleep-stage annotations, and provides multiple physiological channels including electroencephalogram (EEG), electrooculogram (EOG), electromyogram (EMG), respiration, and body temperature. Such data have a typical structure of high-dimensional covariates, repeated observations within subjects, and a natural temporal progression, making them suitable for the application of varying-coefficient modeling.

6.1 Implementation

In our analysis, each overnight recording was treated as one longitudinal trajectory, and only the time interval covered by valid sleep-stage annotations was retained. Since the original EDF files consist of high-frequency continuous waveforms and cannot be directly used in the proposed regression framework, we first performed block-level feature engineering. Specifically, each overnight record was divided into consecutive 5-minute blocks, and only those blocks with at least 80% sleep-stage annotation coverage were kept. For each retained block, physiological features were extracted from multiple channels, and the midpoint of the block was normalized to the interval $[0, 1]$, which represents the relative sleep time within a night. Under the current setting, the final dataset contained 20 overnight records from 10 subjects, yielding a block-level longitudinal dataset.

The response variable was defined as the logarithmically transformed delta-band power (0.5–4 Hz) from the EEG channel `Fpz-Cz`, namely

$$Y_i = \log\{1 + \text{DeltaPower}_i\}.$$

This quantity serves as a continuous measure of slow-wave activity and is well aligned with the varying-coefficient regression framework adopted in this paper.

A total of 12 candidate covariates were constructed. From the EEG channel `Pz-0z`, we extracted the relative band powers in the theta, alpha, sigma, and beta bands, denoted by x_1, x_2, x_3, x_4 , respectively. From the horizontal EOG channel, we extracted the root mean square (RMS) and line length, denoted by x_5, x_6 . From the submental EMG channel, we extracted RMS, denoted by x_7 . From the oro-nasal respiration signal, we extracted the standard deviation and line length, denoted by x_8, x_9 . In addition, rectal temperature, sex, and age were included as x_{10}, x_{11}, x_{12} , respectively. Except for the binary sex indicator, all continuous covariates were standardized before model fitting.

¹<https://www.physionet.org/content/sleep-edfx/1.0.0/>

We then fitted the proposed varying-coefficient model

$$Y_i = \beta_0 + \sum_{k=1}^p X_{ik} \{\mu_k + g_k(t_i)\} + \varepsilon_i, \quad p = 12,$$

where μ_k represents the constant component of the k th covariate effect, and $g_k(t)$ is its time-varying component. To estimate $g_k(t)$, cubic B-spline basis functions were used. Let $B(t)$ denote the centered spline basis vector; then $g_k(t) = B(t)^\top \theta_k$, so that the total effect of the k th covariate is $\beta_k(t) = \mu_k + B(t)^\top \theta_k$. To control smoothness, a second-order difference penalty was imposed on the spline coefficients. At the same time, group sparsity regularization was introduced to distinguish truly time-varying effects from constant effects.

We compared TV-Select with three competing approaches: **VC-Ridge**, **Group-Lasso**, and **Screen+Refit**. The **VC-Ridge** method focuses on smooth estimation of varying effects without emphasizing sparse selection; **Group-Lasso** emphasizes variable screening at the group level but provides less direct smoothness control; and **Screen+Refit** adopts a two-stage strategy of screening followed by refitting. All methods were fitted on the same derived feature set under a unified tuning scheme.

Because the true coefficient functions are unknown for real data, we adopted predictive and structural criteria, including root mean squared error (**RMSE**), mean absolute error (**MAE**), **Roughness** and selection stability (**Stability**). To evaluate generalization ability, we used subject-wise K -fold cross-validation rather than randomly splitting blocks across the whole dataset. In other words, all blocks from the same subject were assigned to either the training set or the test set within a fold. This yields a stricter and more realistic assessment of prediction performance on unseen subjects.

Finally, for the covariates identified as having important time-varying effects, we plotted the estimated coefficient functions $\beta_k(t)$ over normalized sleep time. In the real-data plots, a horizontal line indicates that the corresponding method treats that covariate as having a constant rather than time-varying effect.

6.2 Results

The real-data results are summarized in Table 2. Overall, the TV-Select provides the best predictive performance among the four competing approaches. In particular, it achieves the smallest MAE and RMSE, indicating that it yields the most accurate prediction of the block-level slow-wave activity measure in both absolute deviation and squared-error senses. At the same time, TV-Select also attains the highest Stability value, showing that the set of selected varying effects is much more reproducible across subject-wise data splits. These results suggest that TV-Select strikes a better balance between prediction accuracy and structural reliability than the competing methods.

Table 2: Application results

Method	MAE	RMSE	Roughness	Stability
TV-Select	0.8967	1.1264	0.0693	0.9111
VC-Ridge	1.3555	1.7803	28.2206	0.59
Group-Lasso	1.3557	1.7779	41.7603	0.5
Screen+Refit	1.4007	1.8799	3.9057	0.4116

Another important pattern in Table 2 is the substantial difference in Roughness across methods. TV-Select has by far the smallest Roughness, whereas VC-Ridge and Group-Lasso produce much larger values. Since Roughness measures the degree of fluctuation in the estimated varying-coefficient curves, this indicates that TV-Select yields considerably smoother

temporal effects, while VC-Ridge and Group-Lasso tend to generate much more irregular coefficient trajectories. In real physiological applications, excessively rough curves are difficult to interpret and may reflect overfitting to local noise rather than meaningful time-dependent biological effects. Therefore, the smaller Roughness of TV-Select is not only statistically favorable, but also scientifically desirable.

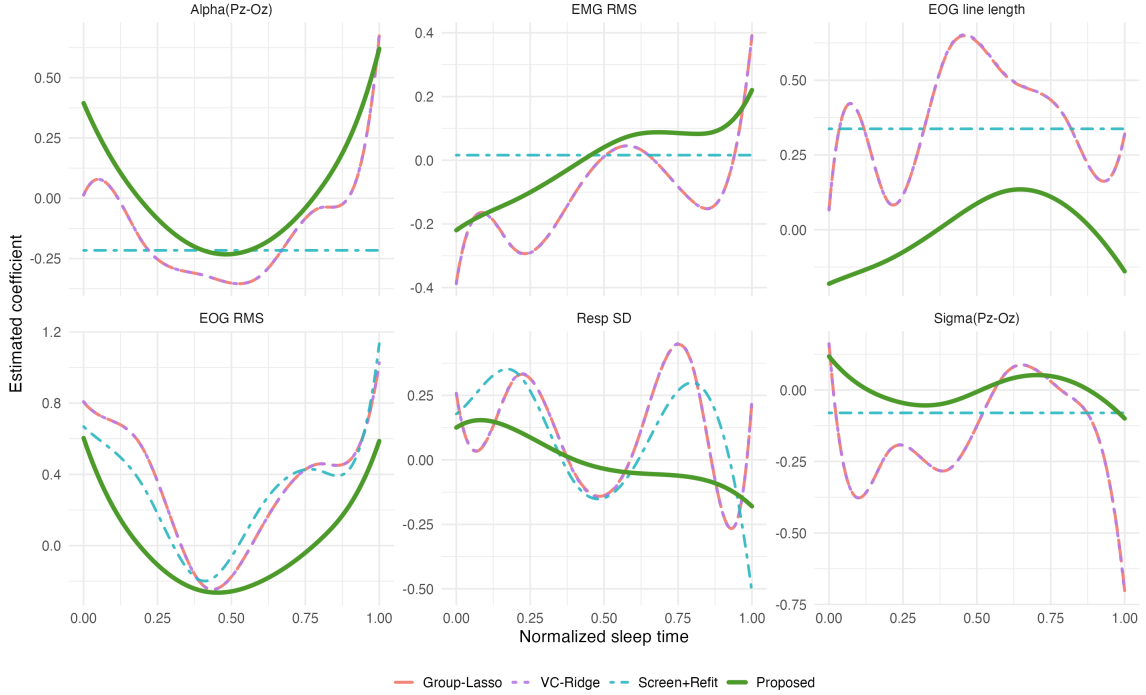


Figure 8: Estimated Time-Varying Effects on Sleep-EDF.

Figure 8 provides further insight into the dynamic effects identified from the Sleep-EDF data. Several variables, including $\text{Alpha}(\text{Pz-Oz})$, $\text{Sigma}(\text{Pz-Oz})$, EOG RMS, EOG line length, EMG RMS, and Resp SD, exhibit clear time-varying patterns under TV-Select. This supports the main modeling assumption of the paper, namely that the effects of physiological covariates on slow-wave activity are not constant over the course of the night. Compared with the competing approaches, the estimated curves from TV-Select are visibly smoother and more coherent over normalized sleep time, whereas the other methods often produce oscillatory or highly unstable patterns. This visual evidence is consistent with the numerical comparison in Table 2.

From a sleep-science perspective, these estimated effects are also plausible. The EEG band-power variables represent different components of cortical oscillatory activity, and their relationships with delta activity are expected to evolve across the night because sleep architecture itself is highly dynamic. For example, the effect of alpha-related activity may vary as the subject moves between lighter sleep and deeper sleep, while sigma activity is closely related to spindle dynamics, which are known to be stage-dependent and modulated over the sleep cycle. Similarly, EOG-derived features reflect eye-movement activity and may carry different information in REM and non-REM periods, while EMG-related variables reflect muscle tone, which also changes systematically as sleep deepens and REM sleep emerges. Respiration variability can likewise be expected to have a nonconstant association with slow-wave activity because autonomic regulation is not uniform throughout the night.

An additional advantage of TV-Select is that its estimated coefficient functions are easier to interpret physiologically. In Figure 8, the competing methods sometimes produce nearly overlapping but highly fluctuating curves, especially for EEG- and respiration-related variables, suggesting sensitivity to local variation in the data. In contrast, TV-Select yields smoother

dynamic trends that are more compatible with the gradual evolution of physiological states during sleep. This is important in practice, because the goal of real-data analysis is not only prediction, but also scientifically meaningful interpretation of how the influence of a physiological feature changes over time.

Taken together, the evidence from both Table 2 and Figure 8 indicates that tTV-Select is preferable for the Sleep-EDF application. It achieves lower prediction error, substantially higher selection stability, and smoother, more interpretable time-varying effects. These findings support the value of combining varying-coefficient modeling with structured regularization when analyzing complex sleep-related physiological data.

7 Conclusion

This paper proposes TV-Select, a unified framework for structural identification in longitudinal varying-coefficient models. By decomposing each coefficient function into a time-invariant mean component and a centered time-varying deviation, the method can distinguish zero, constant, and time-varying effects within a single modeling framework. The doubly penalized formulation combines group sparsity and smoothness regularization, leading to interpretable structure recovery and stable functional estimation. The algorithm is computationally efficient, and the theoretical results establish estimation consistency, recovery of the time-varying set, and oracle-type asymptotic behavior for the constant-effect component after correct structure identification.

The numerical studies and real-data analysis show that TV-Select achieves a favorable balance among structural recovery, smoothness, estimation accuracy, and prediction. Compared with existing methods, it more reliably identifies time-varying effects while avoiding unnecessarily rough coefficient estimates. Several directions remain for future work, including extensions to more general longitudinal response types, more explicit modeling of within-subject dependence, and post-selection inference for the estimated varying effects. These extensions would further broaden the applicability of the TV-Select framework in modern longitudinal studies and

References

- Antoniadis, A., Gijbels, I. and Verhasselt, A. (2012). Variable selection in varying-coefficient models using P-splines. *Journal of Computational and Graphical Statistics* 21: 638–661.
- Bai, J. and Ng, S. (2002). Determining the number of factors in approximate factor models. *Econometrica* 70: 191–221.
- Bai, R., Boland, M. R. and Chen, Y. (2023). Scalable high-dimensional bayesian varying coefficient models with unknown within-subject covariance. *Journal of Machine Learning Research* 24: 1–49.
- Chen, X. and He, Y. (2018). Inference of high-dimensional linear models with time-varying coefficients. *Statistica Sinica* 28: 255–276.
- Dai, R. and Kolar, M. (2021). Inference for high-dimensional varying-coefficient quantile regression. *Electronic Journal of Statistics* 15: 5696–5757.
- Diggle, P., Heagerty, P., Liang, K.-Y. and Zeger, S. L. (2002). *Analysis of Longitudinal Data*. Oxford University Press, 2nd ed.
- Eilers, P. H. C. and Marx, B. D. (1996). Flexible smoothing with B-splines and penalties. *Statistical Science* 11: 89–121.

- Fan, J. and Li, R. (2001). Variable selection via nonconcave penalized likelihood and its oracle properties. *Journal of the American Statistical Association* 96: 1348–1360.
- Fan, J. and Zhang, W. (1999). Statistical estimation in varying coefficient models. *The Annals of Statistics* 27: 1491–1518.
- Hastie, T. and Tibshirani, R. (1993). Varying-coefficient models. *Journal of the Royal Statistical Society: Series B (Methodological)* 55: 757–779.
- Hoover, D. R., Rice, J. A., Wu, C.-L. and Yang, L.-P. (1998). Nonparametric smoothing estimates of time-varying coefficient models with longitudinal data. *Biometrika* 85: 809–822.
- Hu, L., Huang, T. and You, J. (2021). Robust inference in varying-coefficient additive models for longitudinal/functional data. *Statistica Sinica* 31: 773–796.
- Huang, J., Horowitz, J. L. and Wei, F. (2010). Variable selection in nonparametric additive models. *The Annals of Statistics* 38: 2282–2313.
- Hui, F. K. C., Maestrini, L. and Welsh, A. H. (2024). Homogeneity pursuit and variable selection in regression models for multivariate abundance data. *Biometrics* 80: ujad001.
- Kai, B., Li, R. and Zou, H. (2011). New efficient estimation and variable selection methods for semiparametric varying-coefficient partially linear models. *The Annals of Statistics* 39: 305–332.
- Ke, Y., Li, J. and Zhang, W. (2016). Structure identification in panel data analysis. *The Annals of Statistics* 44: 1193–1233.
- Köber, G., Kalisch, R., Puhlmann, L. M. C., Chmitorz, A., Schick, A. and Binder, H. (2023). Deep learning and differential equations for modeling changes in individual-level latent dynamics between observation periods. *Biometrical Journal* 65: e2100381.
- Laird, N. M. and Ware, J. H. (1982). Random-effects models for longitudinal data. *Biometrics* 38: 963–974.
- Li, D., Ke, Y. and Zhang, W. (2015). Model selection and structure specification in ultra-high dimensional generalised semi-varying coefficient models. *The Annals of Statistics* 43: 2676–2705.
- Liang, K.-Y. and Zeger, S. L. (1986). Longitudinal data analysis using generalized linear models. *Biometrika* 73: 13–22.
- Lin, Y. and Zhang, H. H. (2006). Component selection and smoothing in multivariate nonparametric regression. *The Annals of Statistics* 34: 2272–2297.
- Lounici, K., Pontil, M., Geer, S. van de and Tsybakov, A. B. (2011). Oracle inequalities and optimal inference under group sparsity. *The Annals of Statistics* 39: 2164–2204.
- Meier, L., Geer, S. van de and Bühlmann, P. (2008). The group lasso for logistic regression. *Journal of the Royal Statistical Society: Series B (Statistical Methodology)* 70: 53–71.
- Schumaker, L. L. (1981). *Spline Functions: Basic Theory*. John Wiley & Sons.
- Stone, C. J. (1985). Additive regression and other nonparametric models. *The Annals of Statistics* 13: 689–705.
- Tang, Y., Wang, H. J. and Zhu, Z. (2013). Variable selection in quantile varying coefficient models. *Computational Statistics & Data Analysis* 57: 435–449.

- Tibshirani, R. (1996). Regression shrinkage and selection via the lasso. *Journal of the Royal Statistical Society: Series B (Methodological)* 58: 267–288.
- Wang, H. and Leng, C. (2008). A note on adaptive group lasso. *Computational Statistics & Data Analysis* 52: 5277–5286.
- Wang, L., Li, H. and Huang, J. Z. (2008). Variable selection in nonparametric varying-coefficient models. *Journal of the American Statistical Association* 103: 1556–1569.
- Wang, L., Zhou, J. and Qu, A. (2012). Penalized generalized estimating equations for high-dimensional longitudinal data analysis. *Biometrics* 68: 353–360.
- Wei, F., Huang, J. and Li, H. (2011). Variable selection and estimation in high-dimensional varying-coefficient models. *Statistica Sinica* 21: 1515–1540.
- Wu, H. and Zhang, J. T. (2006). *Nonparametric Regression Methods for Longitudinal Data Analysis*. John Wiley & Sons.
- Xue, L., Qu, A. and Zhou, J. (2010). Consistent model selection for marginal generalized additive model. *Journal of the American Statistical Association* 105: 1518–1530.
- Yuan, M. and Lin, Y. (2006). Model selection and estimation in regression with grouped variables. *Journal of the Royal Statistical Society: Series B (Statistical Methodology)* 68: 49–67.
- Zhao, P. and Xue, L. (2011). Variable selection for varying coefficient models with measurement errors. *Metrika* 74: 231–245.
- Zou, H. (2006). The adaptive lasso and its oracle properties. *Journal of the American Statistical Association* 101: 1418–1429.

Proofs of Asymptotic Properties

Notation and Preliminary

Denote the total sample size by $n = \sum_{i=1}^N n_i$. Arrange the observations $\{y_{ij}\}$ into a vector $\mathbf{y} \in \mathbb{R}^n$ and stack the errors $\{\varepsilon_{ij}\}$ analogously to obtain $\boldsymbol{\varepsilon} \in \mathbb{R}^n$. The constant effects $\boldsymbol{\mu} = (\mu_1, \dots, \mu_p)^\top$ are associated with a design matrix $\mathbf{X} \in \mathbb{R}^{n \times p}$, while the spline coefficients $\boldsymbol{\theta}_k \in \mathbb{R}^q$ correspond to block design matrices $\mathbf{Z}_k \in \mathbb{R}^{n \times q}$ for $k = 1, \dots, p$. Concatenating the blocks yields $\mathbf{Z} = [\mathbf{Z}_1, \dots, \mathbf{Z}_p] \in \mathbb{R}^{n \times pq}$ and $\boldsymbol{\theta} = (\boldsymbol{\theta}_1^\top, \dots, \boldsymbol{\theta}_p^\top)^\top$. We use the mixed group norm $\|\boldsymbol{\theta}\|_{2,1} = \sum_{k=1}^p \|\boldsymbol{\theta}_k\|_2$.

Let $\boldsymbol{\theta}_0^*$ denote the spline approximation coefficients from Assumption 3. The resulting approximation error is represented by $\mathbf{r} \in \mathbb{R}^n$ whose entries are

$$r_{ij} = \sum_{k \in \mathcal{S}_{\text{vary}}} x_{ijk} \left\{ g_{0k}(t_{ij}) - \tilde{\mathbf{B}}(t_{ij})^\top \boldsymbol{\theta}_{0k}^* \right\}.$$

With this notation, the stacked model admits the decomposition

$$\mathbf{y} = \beta_0 \mathbf{1}_n + \mathbf{X}\boldsymbol{\mu} + \mathbf{Z}\boldsymbol{\theta} + \boldsymbol{\varepsilon} + \mathbf{r}. \quad (12)$$

The empirical loss takes the form

$$\mathcal{L}(\beta_0, \boldsymbol{\mu}, \boldsymbol{\theta}) = \frac{1}{2n} \|\mathbf{y} - \beta_0 \mathbf{1}_n - \mathbf{X}\boldsymbol{\mu} - \mathbf{Z}\boldsymbol{\theta}\|_2^2,$$

and the penalized criterion is

$$\mathcal{Q}(\beta_0, \boldsymbol{\mu}, \boldsymbol{\theta}) = \mathcal{L}(\beta_0, \boldsymbol{\mu}, \boldsymbol{\theta}) + \lambda_1 \sum_{k=1}^p \|\boldsymbol{\theta}_k\|_2 + \lambda_2 \sum_{k=1}^p \boldsymbol{\theta}_k^\top \boldsymbol{\Omega} \boldsymbol{\theta}_k. \quad (13)$$

Lemma 1 (Spline approximation error). *Under Assumption 3, for each $k \in \mathcal{S}_{\text{vary}}$ there exists $\boldsymbol{\theta}_{0k}^* \in \mathbb{R}^q$ such that*

$$\sup_{t \in [0,1]} \left| g_{0k}(t) - \tilde{\mathbf{B}}(t)^\top \boldsymbol{\theta}_{0k}^* \right| \leq Cq^{-r}.$$

Let $\mathbf{r} \in \mathbb{R}^n$ be the stacked approximation error in (12). If, in addition, $\sup_{i,j,k} \mathbb{E}(x_{ijk}^2) \leq C_x$ and $s_v = |\mathcal{S}_{\text{vary}}|$, then

$$\mathbb{E} \left(\frac{1}{n} \|\mathbf{r}\|_2^2 \right) \leq C s_v q^{-2r}.$$

Moreover, if $\sup_{i,j,k} \|x_{ijk}\|_{\psi_2} \leq K_x$, then there exist constants $c_1, c_2 > 0$ such that with probability at least $1 - c_1(np)^{-c_2}$,

$$\frac{1}{n} \|\mathbf{r}\|_2^2 \leq C s_v q^{-2r} \log(np).$$

Proof. The first display is exactly the spline approximation guarantee in Assumption 3. We now bound $\|\mathbf{r}\|_2^2$.

For each observation (i, j) , define the pointwise spline approximation errors

$$\delta_k(t_{ij}) = g_{0k}(t_{ij}) - \tilde{\mathbf{B}}(t_{ij})^\top \boldsymbol{\theta}_{0k}^*, \quad k \in \mathcal{S}_{\text{vary}}.$$

Then by definition,

$$r_{ij} = \sum_{k \in \mathcal{S}_{\text{vary}}} x_{ijk} \delta_k(t_{ij}).$$

By Assumption 3, $\sup_{i,j} |\delta_k(t_{ij})| \leq Cq^{-r}$ uniformly for each $k \in \mathcal{S}_{\text{vary}}$. Using Cauchy–Schwarz,

$$r_{ij}^2 = \left(\sum_{k \in \mathcal{S}_{\text{vary}}} x_{ijk} \delta_k(t_{ij}) \right)^2 \leq \left(\sum_{k \in \mathcal{S}_{\text{vary}}} x_{ijk}^2 \right) \left(\sum_{k \in \mathcal{S}_{\text{vary}}} \delta_k(t_{ij})^2 \right) \leq \left(\sum_{k \in \mathcal{S}_{\text{vary}}} x_{ijk}^2 \right) s_v C^2 q^{-2r}.$$

Averaging over all (i, j) and taking expectation yields

$$\mathbb{E} \left(\frac{1}{n} \|\mathbf{r}\|_2^2 \right) = \frac{1}{n} \sum_{i,j} \mathbb{E}(r_{ij}^2) \leq \frac{C^2 s_v q^{-2r}}{n} \sum_{i,j} \sum_{k \in \mathcal{S}_{\text{vary}}} \mathbb{E}(x_{ijk}^2) \leq C s_v q^{-2r},$$

where the last inequality uses $\sup_{i,j,k} \mathbb{E}(x_{ijk}^2) \leq C_x$.

For the high-probability bound, sub-Gaussianity implies a uniform tail control. Specifically, since $\|x_{ijk}\|_{\psi_2} \leq K_x$, there exist constants $c, C > 0$ such that

$$\mathbb{P} \left(\max_{i,j,k} |x_{ijk}| > C \sqrt{\log(np)} \right) \leq 2 \exp\{-c \log(np)\} = 2(np)^{-c}.$$

On the event $\mathcal{E}_x = \{\max_{i,j,k} |x_{ijk}| \leq C \sqrt{\log(np)}\}$, we have $\sum_{k \in \mathcal{S}_{\text{vary}}} x_{ijk}^2 \leq s_v \max_k x_{ijk}^2 \leq C s_v \log(np)$ for all (i, j) , and hence

$$r_{ij}^2 \leq C(s_v \log(np)) \cdot (s_v q^{-2r}) = C s_v^2 q^{-2r} \log(np).$$

A slightly sharper bound is obtained by returning to the previous inequality $r_{ij}^2 \leq Cq^{-2r} \sum_{k \in \mathcal{S}_{\text{vary}}} x_{ijk}^2$ and summing over (i, j) :

$$\frac{1}{n} \|\mathbf{r}\|_2^2 \leq Cq^{-2r} \cdot \frac{1}{n} \sum_{i,j} \sum_{k \in \mathcal{S}_{\text{vary}}} x_{ijk}^2 \leq Cq^{-2r} \cdot s_v \max_{i,j,k} x_{ijk}^2 \leq C s_v q^{-2r} \log(np),$$

on \mathcal{E}_x . This proves the stated high-probability inequality. \square

Lemma 2 (Uniform control of noise–design correlations). *Under Assumptions 1–2, suppose in addition that the block designs are well-scaled in the sense that there exists $C_Z > 0$ such that, with probability tending to one,*

$$\max_{1 \leq k \leq p} \left\| \frac{1}{n} \mathbf{Z}_k^\top \mathbf{Z}_k \right\|_{\text{op}} \leq C_Z.$$

Then there exist constants $c_1, c_2 > 0$ such that with probability at least $1 - c_1 p^{-c_2}$,

$$\max_{1 \leq k \leq p} \left\| \frac{1}{n} \mathbf{Z}_k^\top \boldsymbol{\varepsilon} \right\|_2 \leq C \sqrt{\frac{q \log p}{n}}.$$

Proof. Fix $k \in \{1, \dots, p\}$, for any unit vector $\mathbf{u} \in \mathbb{R}^q$ with $\|\mathbf{u}\|_2 = 1$, consider the scalar random variable

$$T_k(\mathbf{u}) = \mathbf{u}^\top \left(\frac{1}{n} \mathbf{Z}_k^\top \boldsymbol{\varepsilon} \right) = \frac{1}{n} \sum_{m=1}^n \left(\mathbf{z}_{k,m}^\top \mathbf{u} \right) \varepsilon_m,$$

where $\mathbf{z}_{k,m}^\top$ denotes the m th row of \mathbf{Z}_k and ε_m is the corresponding stacked error. Conditional on the design, the summands are independent and mean-zero by Assumption 2. Moreover, since ε_m is sub-Gaussian and $\mathbf{z}_{k,m}^\top \mathbf{u}$ is deterministic under conditioning, $T_k(\mathbf{u})$ is sub-Gaussian with

conditional variance proxy bounded by

$$\|T_k(\mathbf{u})\|_{\psi_2} \leq C \frac{K_\varepsilon}{n} \left(\sum_{m=1}^n (\mathbf{z}_{k,m}^\top \mathbf{u})^2 \right)^{1/2} = C \frac{K_\varepsilon}{n} \|\mathbf{z}_k \mathbf{u}\|_2.$$

Using $\|\mathbf{z}_k \mathbf{u}\|_2^2 = \mathbf{u}^\top \mathbf{z}_k^\top \mathbf{z}_k \mathbf{u} \leq \|\mathbf{z}_k^\top \mathbf{z}_k\|_{\text{op}}$ and the scaling condition, we obtain on the high-probability event $\mathcal{E}_Z = \{\|\mathbf{z}_k^\top \mathbf{z}_k/n\|_{\text{op}} \leq C_Z, \forall k\}$ that

$$\|T_k(\mathbf{u})\|_{\psi_2} \leq C \frac{K_\varepsilon}{n} \sqrt{n C_Z} = C \sqrt{\frac{1}{n}}.$$

Hence, conditional on \mathcal{E}_Z , for all $t > 0$,

$$\mathbb{P}(|T_k(\mathbf{u})| > t \mid \mathcal{E}_Z) \leq 2 \exp\{-cnt^2\}. \quad (14)$$

We now upgrade the bound from a fixed direction \mathbf{u} to the Euclidean norm. Let \mathcal{N} be a $1/2$ -net of the unit sphere \mathbb{S}^{q-1} . It is standard that such a net can be chosen with cardinality $|\mathcal{N}| \leq 5^q$ and that

$$\left\| \frac{1}{n} \mathbf{z}_k^\top \boldsymbol{\varepsilon} \right\|_2 \leq 2 \max_{\mathbf{u} \in \mathcal{N}} |T_k(\mathbf{u})|.$$

Therefore, by (14) and a union bound over \mathcal{N} , conditional on \mathcal{E}_Z ,

$$\mathbb{P}\left(\left\| \frac{1}{n} \mathbf{z}_k^\top \boldsymbol{\varepsilon} \right\|_2 > 2t \mid \mathcal{E}_Z\right) \leq |\mathcal{N}| \cdot 2 \exp\{-cnt^2\} \leq 2 \exp\{q \log 5 - cnt^2\}.$$

Choose $t = C \sqrt{(q + \log p)/n}$ with C sufficiently large so that $q \log 5 - cnt^2 \leq -(2 + \delta) \log p$ for some $\delta > 0$. Then we obtain, conditional on \mathcal{E}_Z ,

$$\mathbb{P}\left(\left\| \frac{1}{n} \mathbf{z}_k^\top \boldsymbol{\varepsilon} \right\|_2 > C \sqrt{\frac{q + \log p}{n}} \mid \mathcal{E}_Z\right) \leq 2p^{-(2+\delta)}.$$

Finally, apply a union bound over $k = 1, \dots, p$ to get

$$\mathbb{P}\left(\max_{1 \leq k \leq p} \left\| \frac{1}{n} \mathbf{z}_k^\top \boldsymbol{\varepsilon} \right\|_2 > C \sqrt{\frac{q + \log p}{n}} \mid \mathcal{E}_Z\right) \leq 2p^{-(1+\delta)}.$$

Since $q \lesssim \log p$ in the regime of interest, the bound simplifies to the stated form $C \sqrt{q \log p/n}$. Removing the conditioning and absorbing $\mathbb{P}(\mathcal{E}_Z^c)$ into constants completes the proof. \square

Proof of Theorem 1

Let $(\hat{\beta}_0, \hat{\mu}, \hat{\boldsymbol{\theta}})$ be any minimizer of (13). Define the errors $\Delta_\beta = \hat{\beta}_0 - \beta_0$, $\Delta_\mu = \hat{\mu} - \mu_0$, and $\Delta_\theta = \hat{\boldsymbol{\theta}} - \boldsymbol{\theta}_0^*$. Let $\mathcal{S} = \mathcal{S}_{\text{vary}}$ for brevity.

By optimality of $(\hat{\beta}_0, \hat{\mu}, \hat{\boldsymbol{\theta}})$ and feasibility of $(\beta_0, \mu_0, \boldsymbol{\theta}_0^*)$,

$$\mathcal{Q}(\hat{\beta}_0, \hat{\mu}, \hat{\boldsymbol{\theta}}) \leq \mathcal{Q}(\beta_0, \mu_0, \boldsymbol{\theta}_0^*).$$

Expanding the loss using (12) yields

$$\begin{aligned} \frac{1}{2n} \|\Delta_\beta \mathbf{1}_n + \mathbf{X} \Delta_\mu + \mathbf{Z} \Delta_\theta\|_2^2 &\leq \left\langle \frac{1}{n} \mathbf{Z}^\top (\boldsymbol{\varepsilon} + \mathbf{r}), \Delta_\theta \right\rangle + \left\langle \frac{1}{n} \mathbf{X}^\top (\boldsymbol{\varepsilon} + \mathbf{r}), \Delta_\mu \right\rangle \\ &\quad + \lambda_1 \left(\|\boldsymbol{\theta}_0^*\|_{2,1} - \|\hat{\boldsymbol{\theta}}\|_{2,1} \right) + \lambda_2 \Delta_{\text{ridge}}, \end{aligned} \quad (15)$$

where $\Delta_{\text{ridge}} = \sum_{k=1}^p \left(\boldsymbol{\theta}_{0k}^{*\top} \boldsymbol{\Omega} \boldsymbol{\theta}_{0k}^* - \hat{\boldsymbol{\theta}}_k^\top \boldsymbol{\Omega} \hat{\boldsymbol{\theta}}_k \right) \leq 0$ because $\boldsymbol{\Omega} \succeq 0$ and the ridge term is minimized at $\hat{\boldsymbol{\theta}}$. Hence we may drop $\lambda_2 \Delta_{\text{ridge}}$.

By Cauchy–Schwarz and Lemma 2,

$$\left\langle \frac{1}{n} \mathbf{Z}^\top \boldsymbol{\varepsilon}, \Delta_\theta \right\rangle \leq \max_k \left\| \frac{1}{n} \mathbf{Z}_k^\top \boldsymbol{\varepsilon} \right\|_2 \sum_{k=1}^p \|\Delta_{\theta,k}\|_2 \leq \frac{\lambda_1}{2} \sum_{k=1}^p \|\Delta_{\theta,k}\|_2,$$

for λ_1 chosen as in Assumption 5 with a sufficiently large constant. Similarly, by Lemma 1 and boundedness of the designs,

$$\left| \left\langle \frac{1}{n} \mathbf{Z}^\top \mathbf{r}, \Delta_\theta \right\rangle \right| \leq \frac{1}{n} \|\mathbf{Z}^\top \mathbf{r}\|_{2,\infty} \|\Delta_\theta\|_{2,1} \leq Cq^{-r} \|\Delta_\theta\|_{2,1}.$$

The term involving $\mathbf{X}^\top (\boldsymbol{\varepsilon} + \mathbf{r})$ can be controlled analogously and is of smaller order under the same regime; we absorb it into constants.

Using $\|\boldsymbol{\theta}_0^*\|_{2,1} - \|\hat{\boldsymbol{\theta}}\|_{2,1} \leq \|\Delta_{\theta,S}\|_{2,1} - \|\Delta_{\theta,S^c}\|_{2,1}$, we obtain from (15)

$$\frac{1}{2n} \|\Delta_\beta \mathbf{1}_n + \mathbf{X} \Delta_\mu + \mathbf{Z} \Delta_\theta\|_2^2 \leq \frac{\lambda_1}{2} \|\Delta_\theta\|_{2,1} + \lambda_1 (\|\Delta_{\theta,S}\|_{2,1} - \|\Delta_{\theta,S^c}\|_{2,1}) + Cq^{-r} \|\Delta_\theta\|_{2,1}. \quad (16)$$

For n large and λ_1 dominating q^{-r} (true under $q \asymp n^{1/(2r+1)}$), this implies the cone condition

$$\|\Delta_{\theta,S^c}\|_{2,1} \leq 3\|\Delta_{\theta,S}\|_{2,1}. \quad (17)$$

By Assumption 4 and (17),

$$\frac{1}{n} \|\mathbf{X} \Delta_\mu + \mathbf{Z}_S \Delta_{\theta,S}\|_2^2 \geq \kappa_0 (\|\Delta_\mu\|_2^2 + \|\Delta_{\theta,S}\|_2^2).$$

Moreover, $\|\Delta_{\theta,S}\|_{2,1} \leq \sqrt{s_v} (\sum_{k \in S} \|\Delta_{\theta,k}\|_2^2)^{1/2} \leq \sqrt{s_v} \|\Delta_{\theta,S}\|_2$. Combining with (16) yields

$$\kappa_0 (\|\Delta_\mu\|_2^2 + \|\Delta_{\theta,S}\|_2^2) \leq C\lambda_1 \sqrt{s_v} \|\Delta_{\theta,S}\|_2 + Cs_v q^{-2r}.$$

Hence

$$\|\Delta_\mu\|_2^2 + \|\Delta_{\theta,S}\|_2^2 \leq C (s_v \lambda_1^2 + s_v q^{-2r}).$$

Finally, since each $\boldsymbol{\theta}_k \in \mathbb{R}^q$, $\|\Delta_{\theta,S}\|_2^2 \asymp \sum_{k \in S} \|\Delta_{\theta,k}\|_2^2$ and the displayed bounds in Theorem 1 follow after restoring q -dependence in λ_1 . The L_2 error for \hat{g}_k follows from standard spline basis norm equivalences: $\int_0^1 \{\tilde{\mathbf{B}}(t)^\top \mathbf{v}\}^2 dt \asymp \|\mathbf{v}\|_2^2$ for centered B-splines. \square

Proof of Theorem 2

Denote $\mathcal{S} = \mathcal{S}_{\text{vary}}$ and $\mathcal{S}^c = \{1, \dots, p\} \setminus \mathcal{S}$, let \mathbf{Z}_S denote the concatenation of $\{\mathbf{Z}_k : k \in \mathcal{S}\}$ and $\boldsymbol{\theta}_S$ the stacked vector of $\{\boldsymbol{\theta}_k : k \in \mathcal{S}\}$. For convenience, we work with the scaled objective

$$\mathcal{Q}(\beta_0, \mu, \boldsymbol{\theta}) = \frac{1}{2n} \|\mathbf{y} - \beta_0 \mathbf{1}_n - \mathbf{X} \mu - \mathbf{Z} \boldsymbol{\theta}\|_2^2 + \lambda_1 \sum_{k=1}^p \|\boldsymbol{\theta}_k\|_2 + \lambda_2 \sum_{k=1}^p \boldsymbol{\theta}_k^\top \boldsymbol{\Omega} \boldsymbol{\theta}_k,$$

which is equivalent to (13). The proof uses a primal–dual witness (PDW) construction.

Define the event

$$\mathcal{E} = \left\{ \max_{1 \leq k \leq p} \left\| \frac{1}{n} \mathbf{Z}_k^\top \boldsymbol{\varepsilon} \right\|_2 \leq \frac{\lambda_1}{4} \right\} \cap \left\{ \max_{1 \leq k \leq p} \left\| \frac{1}{n} \mathbf{Z}_k^\top \mathbf{r} \right\|_2 \leq \frac{\lambda_1}{4} \right\},$$

where \mathbf{r} is the spline approximation error vector in (12). Lemma 2 implies $\mathbb{P}(\max_k \|\mathbf{Z}_k^\top \boldsymbol{\varepsilon}/n\|_2 \leq$

$c\sqrt{q \log p/n} \rightarrow 1$, and Lemma 1 implies $\|\mathbf{r}\|_2^2/n \lesssim s_v q^{-2r} \log(np)$, so the same scaling yields $\mathbb{P}(\mathcal{E}) \geq 1 - c_1 p^{-c_2}$ for suitable constants and large n . We prove selection consistency on \mathcal{E} .

Consider the restricted problem in which inactive groups are fixed to zero:

$$(\tilde{\beta}_0, \tilde{\mu}, \tilde{\boldsymbol{\theta}}_{\mathcal{S}}) = \arg \min_{\beta_0, \mu, \boldsymbol{\theta}_{\mathcal{S}}} \left\{ \frac{1}{2n} \|\mathbf{y} - \beta_0 \mathbf{1}_n - \mathbf{X}\mu - \mathbf{Z}_{\mathcal{S}} \boldsymbol{\theta}_{\mathcal{S}}\|_2^2 + \lambda_1 \sum_{k \in \mathcal{S}} \|\boldsymbol{\theta}_k\|_2 + \lambda_2 \sum_{k \in \mathcal{S}} \boldsymbol{\theta}_k^\top \boldsymbol{\Omega} \boldsymbol{\theta}_k \right\}. \quad (18)$$

Define the PDW candidate by

$$\tilde{\boldsymbol{\theta}}_k = \mathbf{0} \quad (k \in \mathcal{S}^c), \quad \tilde{\boldsymbol{\theta}}_{\mathcal{S}} \text{ as in (18)},$$

and take $(\tilde{\beta}_0, \tilde{\mu})$ from (18).

Let the fitted residual under the PDW candidate be

$$\tilde{\mathbf{e}} = \mathbf{y} - \tilde{\beta}_0 \mathbf{1}_n - \mathbf{X}\tilde{\mu} - \mathbf{Z}_{\mathcal{S}} \tilde{\boldsymbol{\theta}}_{\mathcal{S}}.$$

For $k \in \mathcal{S}$, the KKT condition of (18) is

$$-\frac{1}{n} \mathbf{Z}_k^\top \tilde{\mathbf{e}} + 2\lambda_2 \boldsymbol{\Omega} \tilde{\boldsymbol{\theta}}_k + \lambda_1 \tilde{\mathbf{u}}_k = \mathbf{0}, \quad \tilde{\mathbf{u}}_k \in \partial \|\tilde{\boldsymbol{\theta}}_k\|_2. \quad (19)$$

For $k \in \mathcal{S}^c$, to certify that the global optimum of the *full* problem also satisfies $\hat{\boldsymbol{\theta}}_k = \mathbf{0}$, it suffices to show the strict dual feasibility

$$\left\| \frac{1}{n} \mathbf{Z}_k^\top \tilde{\mathbf{e}} \right\|_2 < \lambda_1. \quad (20)$$

Indeed, if (20) holds then we can choose a subgradient $\tilde{\mathbf{u}}_k = \mathbf{Z}_k^\top \tilde{\mathbf{e}} / (n\lambda_1)$ with $\|\tilde{\mathbf{u}}_k\|_2 < 1$, which satisfies the KKT condition for an inactive group at $\hat{\boldsymbol{\theta}}_k = \mathbf{0}$.

Thus, the proof reduces to verifying (20) and then ruling out false negatives (nonzero active blocks).

Using the model decomposition (12),

$$\tilde{\mathbf{e}} = \boldsymbol{\varepsilon} + \mathbf{r} + \mathbf{X}(\mu_0 - \tilde{\mu}) + \mathbf{Z}_{\mathcal{S}}(\boldsymbol{\theta}_{0,\mathcal{S}}^* - \tilde{\boldsymbol{\theta}}_{\mathcal{S}}),$$

where $\boldsymbol{\theta}_{0,\mathcal{S}}^*$ is the spline approximation coefficient vector. Hence, for $k \in \mathcal{S}^c$,

$$\frac{1}{n} \mathbf{Z}_k^\top \tilde{\mathbf{e}} = \underbrace{\frac{1}{n} \mathbf{Z}_k^\top (\boldsymbol{\varepsilon} + \mathbf{r})}_{\text{noise + approximation}} + \underbrace{\frac{1}{n} \mathbf{Z}_k^\top \mathbf{X}(\mu_0 - \tilde{\mu})}_{\text{effect of estimating } \mu} + \underbrace{\frac{1}{n} \mathbf{Z}_k^\top \mathbf{Z}_{\mathcal{S}}(\boldsymbol{\theta}_{0,\mathcal{S}}^* - \tilde{\boldsymbol{\theta}}_{\mathcal{S}})}_{\text{leakage from active groups}}. \quad (21)$$

On the event \mathcal{E} , the first term satisfies

$$\left\| \frac{1}{n} \mathbf{Z}_k^\top (\boldsymbol{\varepsilon} + \mathbf{r}) \right\|_2 \leq \frac{\lambda_1}{2}.$$

It remains to bound the last two terms. This is exactly where the incoherence condition is used. Let $\mathbf{P}_{\mathbf{X}, \mathbf{Z}_{\mathcal{S}}}$ be the projection onto $\text{col}([\mathbf{1}_n, \mathbf{X}, \mathbf{Z}_{\mathcal{S}}])$. Since $(\tilde{\beta}_0, \tilde{\mu}, \tilde{\boldsymbol{\theta}}_{\mathcal{S}})$ solves the restricted problem, the residual $\tilde{\mathbf{e}}$ is orthogonal to the columns of $[\mathbf{1}_n, \mathbf{X}]$ in the least-squares part, and the remaining correlation with $\mathbf{Z}_{\mathcal{S}}$ is controlled by (19). A standard PDW argument (group-lasso analogue) yields

$$\boldsymbol{\theta}_{0,\mathcal{S}}^* - \tilde{\boldsymbol{\theta}}_{\mathcal{S}} = \left(\frac{1}{n} \mathbf{Z}_{\mathcal{S}}^\top (\mathbf{I} - \mathbf{P}_{\mathbf{1}, \mathbf{X}}) \mathbf{Z}_{\mathcal{S}} + 2\lambda_2 \boldsymbol{\Omega}_{\mathcal{S}} \right)^{-1} \left(\frac{1}{n} \mathbf{Z}_{\mathcal{S}}^\top (\mathbf{I} - \mathbf{P}_{\mathbf{1}, \mathbf{X}}) (\boldsymbol{\varepsilon} + \mathbf{r}) - \lambda_1 \tilde{\mathbf{u}}_{\mathcal{S}} \right),$$

where $\tilde{\mathbf{u}}_{\mathcal{S}}$ stacks $\{\tilde{\mathbf{u}}_k : k \in \mathcal{S}\}$. Consequently,

$$\left\| \frac{1}{n} \mathbf{Z}_k^\top (\mathbf{I} - \mathbf{P}_{\mathbf{X}, \mathbf{Z}_{\mathcal{S}}}) \mathbf{Z}_{\mathcal{S}} (\boldsymbol{\theta}_{0, \mathcal{S}}^* - \tilde{\boldsymbol{\theta}}_{\mathcal{S}}) \right\|_2 \leq (1 - \eta) \frac{\lambda_1}{2}$$

for all $k \in \mathcal{S}^c$ on \mathcal{E} , by the incoherence condition stated in Theorem 2. The remaining part involving $\mathbf{Z}_k^\top \mathbf{X}(\mu_0 - \tilde{\mu})/n$ is of the same order and can be absorbed into the same bound under Assumption 4 and the rate in Theorem 1 (its contribution is $o(\lambda_1)$ on \mathcal{E} , since $\|\tilde{\mu} - \mu_0\|_2 = O_p(\sqrt{s_v q} \lambda_1)$ and $\|\mathbf{Z}_k^\top \mathbf{X}/n\|_{\text{op}}$ is bounded). Combining with (21), we obtain on \mathcal{E} that

$$\left\| \frac{1}{n} \mathbf{Z}_k^\top \tilde{\mathbf{e}} \right\|_2 \leq \frac{\lambda_1}{2} + (1 - \eta) \frac{\lambda_1}{2} < \lambda_1,$$

which verifies strict dual feasibility (20) and hence yields $\tilde{\boldsymbol{\theta}}_k = \mathbf{0}$ for all $k \in \mathcal{S}^c$ in the global solution. Therefore, $\widehat{\mathcal{S}}_{\text{vary}} \subseteq \mathcal{S}_{\text{vary}}$ with probability tending to one.

It remains to show that every active group is selected, i.e., $\tilde{\boldsymbol{\theta}}_k \neq \mathbf{0}$ for all $k \in \mathcal{S}$. From the estimation rate in Theorem 1, on an event of probability at least $1 - c_1 p^{-c_2}$,

$$\sum_{k \in \mathcal{S}} \|\tilde{\boldsymbol{\theta}}_k - \boldsymbol{\theta}_{0k}^*\|_2^2 \leq C (s_v q \lambda_1^2 + s_v q^{-2r}).$$

In particular, for each $k \in \mathcal{S}$,

$$\|\tilde{\boldsymbol{\theta}}_k - \boldsymbol{\theta}_{0k}^*\|_2 \leq C (\sqrt{q} \lambda_1 + q^{-r}).$$

Under the growth regime in Assumption 5 and a standard choice of q (e.g., $q \asymp n^{1/(2r+1)}$), the approximation term is dominated and $\sqrt{q} \lambda_1 \asymp \sqrt{q} \sqrt{q \log p/n} = q \sqrt{\log p/n} = o(1)$. The beta-min assumption in Theorem 2 states that $\min_{k \in \mathcal{S}} \|\boldsymbol{\theta}_{0k}^*\|_2 \geq c_0 \lambda_1$ for some $c_0 > 0$. Choosing constants so that $C(\sqrt{q} \lambda_1 + q^{-r}) \leq (c_0/2) \lambda_1$ for large n yields

$$\|\tilde{\boldsymbol{\theta}}_k\|_2 \geq \|\boldsymbol{\theta}_{0k}^*\|_2 - \|\tilde{\boldsymbol{\theta}}_k - \boldsymbol{\theta}_{0k}^*\|_2 \geq c_0 \lambda_1 - \frac{c_0}{2} \lambda_1 = \frac{c_0}{2} \lambda_1 > 0,$$

so every active group remains nonzero. Hence $\mathcal{S} \subseteq \widehat{\mathcal{S}}_{\text{vary}}$ with probability tending to one.

Combining above yields $\mathbb{P}(\widehat{\mathcal{S}}_{\text{vary}} = \mathcal{S}_{\text{vary}}) \rightarrow 1$. \square

Proof of Corollary 1

On the event $\widehat{\mathcal{S}}_{\text{vary}} = \mathcal{S}_{\text{vary}}$, we have $\hat{\boldsymbol{\theta}}_k = \mathbf{0}$ for $k \notin \mathcal{S}_{\text{vary}}$. Then $\hat{\mu}_k$ for such k behaves like an ordinary least squares (or partialled-out) estimator and satisfies

$$\max_{k \notin \mathcal{S}_{\text{vary}}} |\hat{\mu}_k - \mu_{0k}| = O_p \left(\sqrt{\frac{\log p}{n}} \right),$$

by a standard union bound for sub-Gaussian designs. Choosing $\tau_N \asymp \sqrt{\log p/n}$ implies that, for $k \in \mathcal{S}_{\text{zero}}$, $|\hat{\mu}_k| \leq \tau_N$ with probability tending to one, and for $k \in \mathcal{S}_{\text{const}}$, the beta-min condition $|\mu_{0k}| \geq c_1 \tau_N$ ensures $|\hat{\mu}_k| > \tau_N$ with probability tending to one. \square

Proof of Theorem 3

Theorem 3 establishes an oracle asymptotic normality result for the constant effects $\mu_{\mathcal{S}_{\text{const}}}$, conditional on correct identification of the time-varying set.

Let $\mathcal{S} = \mathcal{S}_{\text{vary}}$ and consider the event $\mathcal{A} = \{\widehat{\mathcal{S}}_{\text{vary}} = \mathcal{S}\}$. By Theorem 2, $\mathbb{P}(\mathcal{A}) \rightarrow 1$. On \mathcal{A} , the fitted inactive blocks satisfy $\hat{\boldsymbol{\theta}}_k = \mathbf{0}$ for all $k \notin \mathcal{S}$, so the estimator coincides with the

solution of the restricted problem in (18) (with \mathcal{S} fixed at its true value). In what follows we work under \mathcal{A} and suppress the conditioning notation for brevity.

Partition the constant-effect indices into $\mathcal{S}_{\text{const}}$ and the remaining indices. Write $\mathbf{X}_c = \mathbf{X}_{\mathcal{S}_{\text{const}}}$ and let $\mathbf{W} = [\mathbf{1}_n, \mathbf{X}_{\mathcal{S}}, \mathbf{Z}_{\mathcal{S}}]$ collect all nuisance regressors (intercept, constants associated with time-varying covariates, and the active spline blocks). Define the residual-maker (orthogonal projection complement)

$$\mathbf{M} = \mathbf{I}_n - \mathbf{W}(\mathbf{W}^\top \mathbf{W})^{-1} \mathbf{W}^\top.$$

The key point is that \mathbf{M} removes the influence of the nuisance regressors.

Consider the restricted objective with $\boldsymbol{\theta}_{\mathcal{S}^c} = \mathbf{0}$. For fixed $\boldsymbol{\theta}_{\mathcal{S}}$, the minimizer in $\mu_{\mathcal{S}_{\text{const}}}$ is the OLS solution from regressing $\mathbf{y} - \mathbf{W}\boldsymbol{\gamma}$ on \mathbf{X}_c after partialling out \mathbf{W} , i.e.,

$$\hat{\mu}_c = \left(\mathbf{X}_c^\top \mathbf{M} \mathbf{X}_c \right)^{-1} \mathbf{X}_c^\top \mathbf{M} \mathbf{y} \quad \text{with } \mu_c = \mu_{\mathcal{S}_{\text{const}}}. \quad (22)$$

This identity is a standard consequence of the FWL theorem because μ_c is unpenalized and enters the loss linearly.

Using (12) and the fact that $\mathbf{M}\mathbf{W} = \mathbf{0}$, we obtain

$$\mathbf{M} \mathbf{y} = \mathbf{M} (\mathbf{X}_c \mu_{0,c} + \boldsymbol{\varepsilon} + \mathbf{r}),$$

because the components $\beta_0 \mathbf{1}_n$, $\mathbf{X}_{\mathcal{S}} \mu_{0,\mathcal{S}}$ and $\mathbf{Z}_{\mathcal{S}} \boldsymbol{\theta}_{0,\mathcal{S}}^*$ lie in the column space of \mathbf{W} and are annihilated by \mathbf{M} . Substituting into (22) yields

$$\hat{\mu}_c - \mu_{0,c} = \left(\mathbf{X}_c^\top \mathbf{M} \mathbf{X}_c \right)^{-1} \mathbf{X}_c^\top \mathbf{M} \boldsymbol{\varepsilon} + \left(\mathbf{X}_c^\top \mathbf{M} \mathbf{X}_c \right)^{-1} \mathbf{X}_c^\top \mathbf{M} \mathbf{r}. \quad (23)$$

We now show that the \mathbf{r} term is negligible at the \sqrt{n} scale and derive a CLT for the leading term.

By Cauchy–Schwarz,

$$\left\| \left(\mathbf{X}_c^\top \mathbf{M} \mathbf{X}_c \right)^{-1} \mathbf{X}_c^\top \mathbf{M} \mathbf{r} \right\|_2 \leq \left\| \left(\frac{1}{n} \mathbf{X}_c^\top \mathbf{M} \mathbf{X}_c \right)^{-1} \right\|_{\text{op}} \cdot \left\| \frac{1}{n} \mathbf{X}_c^\top \mathbf{M} \mathbf{r} \right\|_2.$$

Under Assumption 4 (restricted eigenvalue/identifiability), the matrix $(n^{-1} \mathbf{X}_c^\top \mathbf{M} \mathbf{X}_c)$ has eigenvalues bounded away from zero with probability tending to one, so the inverse operator norm is $O_p(1)$. Moreover,

$$\left\| \frac{1}{n} \mathbf{X}_c^\top \mathbf{M} \mathbf{r} \right\|_2 \leq \left\| \frac{1}{n} \mathbf{X}_c^\top \mathbf{r} \right\|_2 \leq \frac{1}{n} \|\mathbf{X}_c\|_{\text{op}} \|\mathbf{r}\|_2.$$

Since $|\mathcal{S}_{\text{const}}|$ is fixed, $\|\mathbf{X}_c\|_{\text{op}} = O_p(\sqrt{n})$ under sub-Gaussian designs. Lemma 1 implies $\|\mathbf{r}\|_2 = O_p(\sqrt{n} q^{-r} \sqrt{s_v})$ (up to log factors). Therefore,

$$\left\| \frac{1}{n} \mathbf{X}_c^\top \mathbf{M} \mathbf{r} \right\|_2 = O_p(q^{-r}), \quad \sqrt{n} \left\| \left(\mathbf{X}_c^\top \mathbf{M} \mathbf{X}_c \right)^{-1} \mathbf{X}_c^\top \mathbf{M} \mathbf{r} \right\|_2 = o_p(1),$$

provided $q^r/\sqrt{n} \rightarrow \infty$, which is satisfied under the standard spline regime (e.g., $q \asymp n^{1/(2r+1)}$ with $r > 2$). Hence the approximation error does not affect the \sqrt{n} limit distribution.

Fix any vector $\mathbf{a} \in \mathbb{R}^{|\mathcal{S}_{\text{const}}|}$. Multiply (23) by $\sqrt{n} \mathbf{a}^\top$ and ignore the $o_p(1)$ term from above:

$$\sqrt{n} \mathbf{a}^\top (\hat{\mu}_c - \mu_{0,c}) = \mathbf{a}^\top \left(\frac{1}{n} \mathbf{X}_c^\top \mathbf{M} \mathbf{X}_c \right)^{-1} \left(\frac{1}{\sqrt{n}} \mathbf{X}_c^\top \mathbf{M} \boldsymbol{\varepsilon} \right) + o_p(1).$$

Define the n -dimensional vector

$$\mathbf{v} = \mathbf{M}\mathbf{X}_c \left(\frac{1}{n} \mathbf{X}_c^\top \mathbf{M}\mathbf{X}_c \right)^{-1} \mathbf{a},$$

so that

$$\mathbf{a}^\top \left(\frac{1}{n} \mathbf{X}_c^\top \mathbf{M}\mathbf{X}_c \right)^{-1} \left(\frac{1}{\sqrt{n}} \mathbf{X}_c^\top \mathbf{M}\boldsymbol{\varepsilon} \right) = \frac{1}{\sqrt{n}} \mathbf{v}^\top \boldsymbol{\varepsilon} = \frac{1}{\sqrt{n}} \sum_{m=1}^n v_m \varepsilon_m.$$

Conditional mean zero follows from Assumption 2. Moreover, by standard operator-norm bounds under Assumption 4 and fixed $|\mathcal{S}_{\text{const}}|$, $\max_m |v_m| = o_p(\sqrt{n})$ and $\|\mathbf{v}\|_2^2/n \rightarrow \mathbf{a}^\top \mathbf{V}^{-1} \mathbf{a}$, where

$$\mathbf{V} = \lim_{N \rightarrow \infty} \frac{1}{n} \mathbf{X}_c^\top \mathbf{M}\mathbf{X}_c,$$

which is positive definite. Therefore, by the Lindeberg–Feller central limit theorem for triangular arrays (or Lyapunov’s condition using sub-Gaussianity),

$$\frac{1}{\sqrt{n}} \sum_{m=1}^n v_m \varepsilon_m \xrightarrow{d} \mathcal{N}\left(0, \sigma^2 \mathbf{a}^\top \mathbf{V}^{-1} \mathbf{a}\right),$$

and Slutsky’s theorem gives

$$\sqrt{n} \mathbf{a}^\top (\hat{\mu}_{\mathcal{S}_{\text{const}}} - \mu_{0, \mathcal{S}_{\text{const}}}) \xrightarrow{d} \mathcal{N}\left(0, \sigma^2 \mathbf{a}^\top \mathbf{V}^{-1} \mathbf{a}\right).$$

This is exactly the oracle limit distribution claimed in Theorem 3. □